Multi-Tenant C-RAN With Spectrum Pooling: Downlink Optimization Under Privacy Constraints

Seok-Hwan Park, *Member, IEEE*, Osvaldo Simeone, *Fellow, IEEE*, and Shlomo Shamai, *Fellow, IEEE*

***Abstract*—Spectrum pooling allows multiple operators, or tenants, to share the same frequency bands. This paper studies the optimization of spectrum pooling for the downlink of a multi-tenant cloud radio access network system in the presence of inter-tenant privacy constraints. The spectrum available for downlink transmission is partitioned into private and shared subbands, and the participating operators cooperate to serve the user equipment (UEs) on the shared subband. The network of each operator consists of a cloud processor (CP) that is connected to proprietary radio units (RUs) by means of finite-capacity fronthaul links. In order to enable inter-operator cooperation, the CPs of the participating operators are also connected by finite-capacity backhaul links. Inter-operator cooperation may, hence, result in loss of privacy. Fronthaul and backhaul links are used to transfer quantized baseband signals. Standard quantization is considered first. Then, a novel approach based on the idea of correlating quantization noise signals across RUs of different operators is proposed to control the trade-off between distortion at UEs and inter-operator privacy. The problem of optimizing the bandwidth allocation, precoding, and fronthaul/backhaul compression strategies is tackled under constraints on backhaul and fronthaul capacity, as well as on per-RU transmit power and inter-operator privacy. For both cases, the optimization problems are tackled using the concave convex procedure, and extensive numerical results are provided.**

***Index Terms*—C-RAN, multi-tenant, spectrum pooling, RAN sharing, privacy constraint, precoding, fronthaul compression, multivariate compression.**

I. Introduction

SPECTRUM pooling among multiple network operators, or tenants, is an emerging technique for meeting the rapidly increasing traffic demands over the available scarce spectrum resources [1]–[6]. Spectrum pooling can be implemented by means of orthogonal or non-orthogonal resource allocation. In orthogonal spectrum pooling, the frequency channels are exclusively, but dynamically, allocated to the participating operators [2]. In contrast, with non-orthogonal spectrum pooling, parts of the spectrum can be shared between operators. In addition to spectrum pooling, radio access network (RAN) sharing, whereby RAN infrastructure nodes are shared by the tenants, has also been considered [4], [5]. RAN sharing and spectrum pooling are two examples of network slicing, a key technology for the upcoming 5G wireless systems [3], [7].

In a Cloud RAN (C-RAN) architecture, a Cloud Processor (CP) carries out centralized baseband signal processing on behalf of a number of the connected Radio Units (RUs). The CP communicates quantized baseband signals over fronthaul links, while the RUs only perform radio frequency functionalities [8], [9]. Motivated by the promised reduction in capital and operational expenditures, the C-RAN technology is currently being deployed for testing. In this paper, we focus on the optimization of spectrum pooling across multiple tenants in a C-RAN architecture, as illustrated in Fig. 1.

Existing papers on C-RAN downlink optimization, such as [10]–[16], have focused on single-tenant systems. These works, and related references, study the design of coordinated precoding and fronthaul compression strategies. Specifically, references [10], [15], [16] consider the use of standard point-to-point fronthaul compression and quantization strategies, whereas [11], [12], [14] investigate a more advanced approach based on multivariate compression and quantization. These perform the joint compression and quantization of baseband signals across multiple RUs, with the aim of controlling the impact of quantization distortion at the user equipment (UEs). Dual approaches for the uplink of C-RAN were studied in, e.g., [17], [18]. We refer to [8], [9] for a comprehensive review.

Tackling the optimization of C-RAN systems in the presence of multiple operators presents novel optimization degrees of freedom and technical challenges. As a key novel design dimension, the available bandwidth may be optimally split into private and shared subbands, where the private subbands are exclusively used by the respective operators while the shared subband is shared by all the participating operators (see Fig. 2). Furthermore, cooperation and coordination on the shared subband are facilitated by communication between the CPs, which requires the design of the signals exchanged on the inter-CP interface as a function of the inter-CP capacity. Finally, the

Manuscript received October 17, 2017; revised April 5, 2018 and July 14, 2018; accepted August 10, 2018. Date of publication August 15, 2018; date of current version November 12, 2018. The work of S.-H. Park was supported by the National Research Foundation of Korea (NRF) grants funded by the Korea government under Grants NRF-2015R1C1A1A01051825 and NRF-2018R1D1A1B07040322. The work of O. Simeone was supported in part by the U.S. NSF under Grant 1525629 and by the European Research Council (ERC) under the European Union's Horizon 2020 research and innovation programme under Grant 725731. The work of S. Shamai has been supported by the European Union's Horizon 2020 Research and Innovation Programme under Grant 694630. This paper was presented in part at the IEEE International Workshop on Signal Processing Advances in Wireless Communications (SPAWC), Kalamata, Greece, June 2018. The review of this paper was coordinated by Dr. Y. Ji. *(Corresponding author: Seok-Hwan Park.)*

S.-H. Park is with the Division of Electronic Engineering, Chonbuk National University, Jeonju 54896, South Korea (e-mail: seokhwan@jbnu.ac.kr).

O. Simeone is with the Department of Informatics, King's College London, London WC2R 2LS, U.K. (e-mail: osvaldo.simeone@kcl.ac.uk).

S. Shamai is with the Department of Electrical Engineering, Technion, Haifa 32000, Israel (e-mail: sshlomo@ee.technion.ac.il).

Color versions of one or more of the figures in this paper are available online at http://ieeexplore.ieee.org.

Digital Object Identifier 10.1109/TVT.2018.2865599

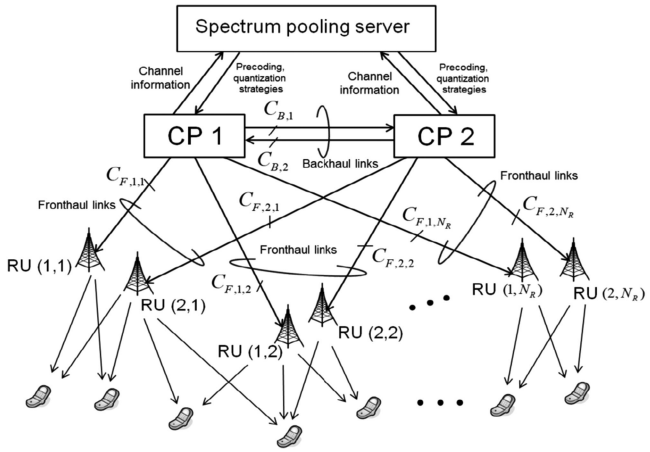

Fig. 1. Illustration of the downlink of a multi-tenant C-RAN system.

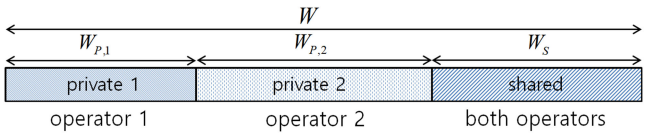

Fig. 2. Illustration of frequency band splitting for the downlink transmission into private and shared bands.

optimization problem entails a trade-off between the benefits accrued from inter-operator cooperation and the amount of information exchanged about the respective users' data.

In this paper, we study the design of the mult-tenant C-RAN system illustrated in Fig. 1 under the assumption that fronthaul and inter-CP backhaul links carry quantized baseband signals. Note that this is the standard mode of operation for C-RAN CP-to-RUs links. We tackle the joint optimization of bandwidth allocation and of precoding and quantization strategies under constraints on fronthaul and backhaul capacity and privacy for the inter-CP communications.

To this end, we first consider standard point-to-point quantization as in most prior work on C-RAN. Then, a novel quantization scheme based on multivariate compression [11], [14] is proposed. Through this approach, the CP of an operator is able to correlate the quantization noise signals across the RUs of *both* operators, so as to better control the trade-off between the distortion observed by the UEs and inter-operator privacy. Note that the crucial element of inter-operator privacy was not present in prior works [11], [12], [14]. In this regard, we note that the CP and RUs of one operator act as untrusted relays for the other operators, and hence the proposed technique can also be applied for the relay channels with untrusted relays studied in [19], [20]. We remark that the proposed physical layer security approach is unconditionally secure, rather than computationally secure as conventional cryptographic methods. Furthermore, it can be directly implemented using baseband processing by designing the fronthaul quantizers at the CPs without requiring additional encryption and decryption mechanisms. Finally, the proposed system can be generalized so as to include also cryptographic operations at higher layers on top of the physical layer (see, e.g., [21]).

The rest of the paper is organized as follows. The system model is described in Sec. II, and Sec. III presents the operation of the multi-tenant C-RAN system with spectrum pooling. We discuss the optimization of the multi-tenant C-RAN system in Sec. IV. The novel multivariate compression scheme is introduced in Sec. V. We provide numerical results that validate the advantages of optimized spectrum pooling and of multivariate compression in Sec. VI, and the paper is concluded in Sec. VII.

Some notations used throughout the paper are summarized as follows. The mutual information between the random variables X and Y is denoted as $I(X;Y)$, and $h(X|Y)$ denotes the conditional differential entropy of X given Y. We use the notation $\mathcal{CN}(\boldsymbol{\mu}, \mathbf{R})$ to denote the circularly symmetric complex Gaussian distribution with mean $\boldsymbol{\mu}$ and covariance matrix $\mathbf{R}$. The set of all $M \times N$ complex matrices is denoted by $\mathbb{C}^{M\times N}$, and $\mathtt{E}(\cdot)$ represents the expectation operator. The operation $(\cdot)^\dagger$ denotes Hermitian transpose of a matrix or vector.

II. System Model

We consider the downlink of a multi-tenant C-RAN with N_O operators. As shown in Fig. 1, we focus on the case of $N_O = 2$ operators, but the treatment could be generalized for any N_O at the cost of a more cumbersome notation. We assume that each operator has a single CP, N_R RUs and N_U UEs. We denote the rth RU and the kth UE of the ith operator as RU (i,r) and UE (i,k), respectively. We consider a general MIMO set-up in which RU (i,r) and UE (i,k) have $n_{R,i,r}$ and $n_{U,i,k}$ antennas, respectively, and define the number $n_{R,i} \triangleq \sum_{r\in\mathcal{N}_R} n_{R,i,r}$ of total RU antennas of each operator. The sets of RU and UE indices for either operator are denoted as $\mathcal{N}_R \triangleq \{1,2,\ldots,N_R\}$ and $\mathcal{N}_U \triangleq \{1,2,\ldots,N_U\}$, respectively, while $\mathcal{N}_O \triangleq \{1,2\}$ is the set of operator indices.

The CP of each operator i, indicated as CP i, has a message $M_{i,k} \in \{1,2,\ldots,2^{nR_{i,k}}\}$ to deliver to UE (i,k), where n is the coding block length, assumed to be sufficiently large, and $R_{i,k}$ denotes the rate of the message $M_{i,k}$ in bits per second (bit/s).

As in related works for C-RAN systems (see, e.g., [10]–[12]), we assume that CP i is connected to RU (i,r) by a *fronthaul link* of capacity $C_{F,i,r}$ bit/s. In addition, in order to enable inter-operator cooperation, we assume that, as suggested in [4], the CPs of two operators are connected to each other. Specifically, CP i can send information to the other CP $\bar{i}$ on a *backhaul link* of capacity $C_{B,i}$ bit/s, where $\bar{i}$ indicates $\bar{i} = 3 - i$, i.e., $\bar{1} = 2$ and $\bar{2} = 1$. We note that it would be generally useful to deploy interfaces between the RUs of different operators [4], but this work focuses on investigating the advantages of inter-CP connections only.

Inter-operator cooperation via RAN sharing, as enabled by the inter-CP backhaul links, may cause information leakage from one operator to the other, which may degrade the confidentiality of the UE messages. When designing the multi-tenant C-RAN system, we will hence impose privacy constraints such that the

inter-operator information leakage rate does not exceed a given tolerable threshold value.

We assume flat-fading channel models, and divide the downlink bandwidth as shown in Fig. 2 into private and shared subbands. The signal $\mathbf{y}_{i,k}^{(i)} \in \mathbb{C}^{n_{U,i,k}\times 1}$ received by UE (i,k) on private subband i can be written as

$$\mathbf{y}_{i,k}^{(i)} = \sum_{r\in\mathcal{N}_R} \mathbf{H}_{i,k}^{i,r}\mathbf{x}_{i,r}^{(i)} + \mathbf{z}_{i,k}^{(i)}, \tag{1}$$

where $\mathbf{H}_{i,k}^{j,r} \in \mathbb{C}^{n_{U,i,k}\times n_{R,j,r}}$ represents the channel matrix from RU (j,r) to UE (i,k); $\mathbf{x}_{i,r}^{(i)} \in \mathbb{C}^{n_{R,i,r}\times 1}$ is the signal transmitted by RU (i,r) on the private subband i; and $\mathbf{z}_{i,k}^{(i)} \sim \mathcal{CN}(\mathbf{0},\mathbf{I})$ denotes the additive noise. Similarly, the signal $\mathbf{y}_{i,k}^{(S)} \in \mathbb{C}^{n_{U,i,k}\times 1}$ received by UE (i,k) on the shared subband is given as

$$\mathbf{y}_{i,k}^{(S)} = \sum_{r\in\mathcal{N}_R} \mathbf{H}_{i,k}^{i,r}\mathbf{x}_{i,r}^{(S)} + \sum_{r\in\mathcal{N}_R} \mathbf{H}_{i,k}^{\bar{i},r}\mathbf{x}_{\bar{i},r}^{(S)} + \mathbf{z}_{i,k}^{(S)}, \tag{2}$$

where $\mathbf{x}_{i,r}^{(S)} \in \mathbb{C}^{n_{R,i,r}\times 1}$ is the signal transmitted by RU (i,r) on the shared subband; and $\mathbf{z}_{i,k}^{(S)} \sim \mathcal{CN}(\mathbf{0},\mathbf{I})$ is the additive noise.

As illustrated in Fig. 1, in a manner similar to, e.g., [4], [22]–[24], we assume that there is a spectrum pooling server that carries out the centralized optimization of the signal processing strategies, that determine spectrum sharing on behalf of the two operators. For this purpose, the server needs to have the knowledge of the channel matrices $\{\mathbf{H}_{i,k}^{j,r}\}_{i,j\in\mathcal{N}_O, r\in\mathcal{N}_R, k\in\mathcal{N}_U}$, inter-CP backhaul links' capacity $\{C_{B,i}\}_{i\in\mathcal{N}_O}$ and CP-to-RUs fronthaul links' capacity $\{C_{F,i,r}\}_{i\in\mathcal{N}_O, r\in\mathcal{N}_R}$. In this work, as in [25, Sec. II-C], we focus on a slow-fading environment so that the overhead for acquiring accurate CSI is negligible. However, in practice, CSI available at the spectrum pooling server may not be perfect due to both channel estimation errors and distortions related to the communication between the CPs and the server. Nevertheless, imperfect CSI can be accounted for by using standard methods that have been widely investigated considering either a deterministic worst-case model as in, e.g., [26] or a stochastic model as in, e.g., [27]. We leave a full investigation of this aspect to future research in order to focus in this work on the key aspects of multi-tenancy and privacy. Furthermore, we assume that each RU uses Non-Orthogonal Multiple Access (NOMA), which is known to be information-theoretically superior to the orthogonal allocation of resources to users in the same cell [28]–[30].

III. Multi-Tenant C-RAN With Spectrum Pooling

In this section, we describe the operation of the multi-tenant C-RAN system with spectrum pooling and RAN infrastructure sharing by means of inter-CP connections.

A. Overview

As illustrated in Fig. 2, we split the frequency band of bandwidth W [Hz] into three subbands, where the first two subbands are exclusively used by the respective operators, while the last subband is shared by both operators. Accordingly, the bandwidth W is decomposed as

$$W = W_{P,1} + W_{P,2} + W_S, \tag{3}$$

where $W_{P,i}$ is the bandwidth of the private subband assigned to operator i, and W_S is the bandwidth of the shared subband.

The private subbands are used by each operator to communicate to their respective UEs with no interference from the other operators' RUs using standard fronthaul-enabled C-RAN transmission [8]. In contrast, the shared subband is used simultaneously by the two operators, which can coordinate their transmission through the inter-CP links. In the following, we detail the operation of CPs, RUs and UEs.

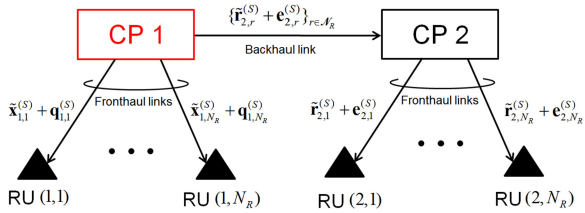

Fig. 3. Illustration of fronthaul and backhaul quantization at CP 1.

B. Encoding at CPs

In order to enable transmission over the private and shared subbands, we split the message $M_{i,k}$ intended for each UE (i,k) into two submessages $M_{i,k,P}$ and $M_{i,k,S}$ of rates $R_{i,k,P}$ and $R_{i,k,S}$, respectively, with $R_{i,k,P} + R_{i,k,S} = R_{i,k}$. The submessages $M_{i,k,P}$ and $M_{i,k,S}$ are communicated to the UE (i,k) on the private and shared subbands, respectively. Each submessage $M_{i,k,m}$, $m \in \{P,S\}$, is encoded by CP i in a baseband signal $\mathbf{s}_{i,k,m} \in \mathbb{C}^{d_{i,k,m}\times 1}$. We consider standard random coding with Gaussian codebooks, and hence each symbol $\mathbf{s}_{i,k,m}$ is distributed as $\mathbf{s}_{i,k,m} \sim \mathcal{CN}(\mathbf{0},\mathbf{I})$.

1) Linear Precoding for Private Subband: CP i linearly precodes the signals $\{\mathbf{s}_{i,k,P}\}_{k\in\mathcal{N}_U}$ to be transmitted on the private subband as

$$\tilde{\mathbf{x}}_i^{(i)} = \left[\tilde{\mathbf{x}}_{i,1}^{(i)\dagger} \cdots \tilde{\mathbf{x}}_{i,N_R}^{(i)\dagger}\right]^\dagger = \sum_{k\in\mathcal{N}_U} \mathbf{V}_{i,k}^{(i)}\mathbf{s}_{i,k,P}, \tag{4}$$

where the subvector $\tilde{\mathbf{x}}_{i,r}^{(i)} \in \mathbb{C}^{n_{R,i,r}\times 1}$ is to be transferred to RU (i,r) on the fronthaul link, and $\mathbf{V}_{i,k}^{(i)} \in \mathbb{C}^{n_{R,i}\times d_{i,k,P}}$ is the precoding matrix for the signal $\mathbf{s}_{i,k,P}$.

2) Linear Precoding for Shared Subband: On the shared subband, the CPs and RUs of both operators are activated to cooperatively serve all the UEs. To this end, CP i precodes the signal $\mathbf{s}_{i,k,S}$ for each UE (i,k) into two precoded signals: signal $\tilde{\mathbf{x}}_i^{(S)} \in \mathbb{C}^{n_{R,i}\times 1}$ to be transmitted by its RUs and signal $\tilde{\mathbf{r}}_{\bar{i}}^{(S)} \in \mathbb{C}^{n_{R,\bar{i}}\times 1}$ to be sent by the other operator $\bar{i}$. This is illustrated in Fig. 3. As we will discuss, the transmission through the RUs of the other operator is enabled by the inter-CP backhaul link and is subject to privacy constraints.

Mathematically, we write the precoded signals in the shared subband as

$$\tilde{\mathbf{x}}_i^{(S)} = \left[\tilde{\mathbf{x}}_{i,1}^{(S)\dagger} \cdots \tilde{\mathbf{x}}_{i,N_R}^{(S)\dagger}\right]^\dagger = \sum_{k\in\mathcal{N}_U} \mathbf{V}_{i,k}^{(S)} \mathbf{s}_{i,k,S}, \quad (5)$$

$$\tilde{\mathbf{r}}_{\bar{i}}^{(S)} = \left[\tilde{\mathbf{r}}_{\bar{i},1}^{(S)\dagger} \cdots \tilde{\mathbf{r}}_{\bar{i},N_R}^{(S)\dagger}\right]^\dagger = \sum_{k\in\mathcal{N}_U} \mathbf{T}_{\bar{i},k}^{(S)} \mathbf{s}_{i,k,S}, \quad (6)$$

where the subvectors $\tilde{\mathbf{x}}_{i,r}^{(S)} \in \mathbb{C}^{n_{R,i,r}\times 1}$ and $\tilde{\mathbf{r}}_{\bar{i},r}^{(S)} \in \mathbb{C}^{n_{R,\bar{i},r}\times 1}$ are communicated to the RUs (i,r) and $(\bar{i},r)$, respectively; and $\mathbf{V}_{i,k}^{(S)} \in \mathbb{C}^{n_{R,i}\times d_{i,k,S}}$ and $\mathbf{T}_{\bar{i},k}^{(S)} \in \mathbb{C}^{n_{R,\bar{i}}\times d_{i,k,S}}$ are the precoding matrices for the signal $\mathbf{s}_{i,k,S}$ associated with the RUs (i,r) and $(\bar{i},r)$, respectively.

3) Fronthaul Compression: CP i is directly connected to the RUs (i,r) in its network via fronthaul links. Therefore, following the standard C-RAN operation, the CP i quantizes the precoded signals $\tilde{\mathbf{x}}_{i,r}^{(i)}$ and $\tilde{\mathbf{x}}_{i,r}^{(S)}$ for transmission on the fronthaul link to RU (i,r) on private and shared subbands. Assuming vector quantization, we model the quantized signals $\hat{\mathbf{x}}_{i,r}^{(m)}$, $m \in \{i,S\}$, as

$$\hat{\mathbf{x}}_{i,r}^{(m)} = \tilde{\mathbf{x}}_{i,r}^{(m)} + \mathbf{q}_{i,r}^{(m)}, \quad (7)$$

where $\mathbf{q}_{i,r}^{(m)}$ represents the quantization noise. Adopting a Gaussian test channel as in [10]–[12], the quantization noise $\mathbf{q}_{i,r}^{(m)}$ is independent of the precoded signal $\tilde{\mathbf{x}}_{i,r}^{(m)}$ and distributed as $\mathbf{q}_{i,r}^{(m)} \sim \mathcal{CN}(\mathbf{0}, \mathbf{\Omega}_{i,r}^{(m)})$. We recall that a Gaussian test channel can be well approximated by vector lattice quantizers [31].

We first adopt standard point-to-point compression, whereby the signals $\{\tilde{\mathbf{x}}_{i,r}^{(m)}\}_{r\in\mathcal{N}_R, m\in\{i,S\}}$ for different RUs and subbands are compressed independently. A more sophisticated approach based on multivariate compression will be discussed in Sec. V. Accordingly, with point-to-point compression, the rate, in bit/s, needed to send $\hat{\mathbf{x}}_{i,r}^{(m)}$ to RU (i,r) is given as $W_{i,m} I(\tilde{\mathbf{x}}_{i,r}^{(m)}; \hat{\mathbf{x}}_{i,r}^{(m)})$ [32, Ch. 3], where the mutual information $I(\tilde{\mathbf{x}}_{i,r}^{(m)}; \hat{\mathbf{x}}_{i,r}^{(m)})$ can be written as

$$I\left(\tilde{\mathbf{x}}_{i,r}^{(m)}; \hat{\mathbf{x}}_{i,r}^{(m)}\right) = g_{i,r}^{(m)}\left(\mathbf{V}, \mathbf{\Omega}\right) = \Phi\left(\sum_{k\in\mathcal{N}_U} \mathbf{K}\left(\mathbf{E}_{i,r}^\dagger \mathbf{V}_{i,k}^{(m)}\right), \mathbf{\Omega}_{i,r}^{(m)}\right). \quad (8)$$

Here we defined the functions

$$\Phi(\mathbf{A},\mathbf{B}) = \log_2 \det(\mathbf{A}+\mathbf{B}) - \log_2 \det(\mathbf{B}), \quad (9)$$

and $\mathbf{K}(\mathbf{A}) = \mathbf{A}\mathbf{A}^\dagger$; the shaping matrix $\mathbf{E}_{i,r} \in \mathbb{C}^{n_{R,i}\times n_{R,i,r}}$ that has all-zero elements except the rows from $\sum_{q=1}^{r-1} n_{R,i,q} + 1$ to $\sum_{q=1}^{r} n_{R,i,q}$ which contains an identity matrix; and the notation $W_{i,m} = W_{P,i}\cdot 1(m=i) + W_S \cdot 1(m=S)$. Here $1(\cdot)$ represents the indicator function that returns 1 if the input argument is true and 0 otherwise.

4) Backhaul Compression: As seen in Fig. 3, since there is no direct link between CP i and the RUs $(\bar{i},r)$ of the other tenant, CP i sends the precoded signal $\tilde{\mathbf{r}}_{\bar{i},r}^{(S)}$ to the RU $(\bar{i},r)$ through CP $\bar{i}$. The CP $\bar{i}$ forwards the received bit stream from CP i to RU $(\bar{i},r)$. Since both the backhaul link from CP i to CP $\bar{i}$ and the fronthaul link from CP $\bar{i}$ to RU $(\bar{i},r)$ have finite capacities, CP i quantizes the signal $\tilde{\mathbf{r}}_{\bar{i},r}^{(S)}$ to obtain the quantized signal

$$\mathbf{r}_{\bar{i},r}^{(S)} = \tilde{\mathbf{r}}_{\bar{i},r}^{(S)} + \mathbf{e}_{\bar{i},r}^{(S)}, \quad (10)$$

where $\mathbf{e}_{\bar{i},r}^{(S)}$ represents the quantization noise. Using the same quantization model discussed above, this is distributed as $\mathbf{e}_{\bar{i},r}^{(S)} \sim \mathcal{CN}(\mathbf{0}, \mathbf{\Sigma}_{\bar{i},r}^{(S)})$. As mentioned, we assume here the independent compression of the signals $\{\tilde{\mathbf{r}}_{\bar{i},r}^{(S)}\}_{r\in\mathcal{N}_R}$ for different RUs, so that the rate needed to convey each signal $\mathbf{r}_{\bar{i},r}^{(S)}$ is given as $W_S I(\tilde{\mathbf{r}}_{\bar{i},r}^{(S)}; \mathbf{r}_{\bar{i},r}^{(S)})$, with

$$I\left(\tilde{\mathbf{r}}_{\bar{i},r}^{(S)}; \mathbf{r}_{\bar{i},r}^{(S)}\right) = \gamma_{\bar{i},r}^{(S)}\left(\mathbf{T}, \mathbf{\Sigma}\right) = \Phi\left(\sum_{k\in\mathcal{N}_U} \mathbf{K}\left(\mathbf{E}_{\bar{i},r}^\dagger \mathbf{T}_{\bar{i},k}^{(S)}\right), \mathbf{\Sigma}_{\bar{i},r}^{(S)}\right). \quad (11)$$

The capacity constraint for the backhaul link from CP i to CP $\bar{i}$ can be written as

$$\sum_{r\in\mathcal{N}_R} W_S \gamma_{\bar{i},r}^{(S)}\left(\mathbf{T}, \mathbf{\Sigma}\right) \le C_{B,i},\ i \in \mathcal{N}_O, \quad (12)$$

since the backhaul link needs to carry the baseband signals for all the RUs. Similarly, the capacity constraint for the fronhtaul link from CP i to RU (i,r) can be expressed as

$$\sum_{m\in\{i,S\}} W_{i,m} g_{i,r}^{(m)}\left(\mathbf{V}, \mathbf{\Omega}\right) + W_S \gamma_{i,r}^{(S)}\left(\mathbf{T}, \mathbf{\Sigma}\right) \le C_{F,i,r}, \quad (13)$$

for $i \in \mathcal{N}_O$, $r \in \mathcal{N}_R$, since the fronthaul link needs to support transmission of the signals for both private and shared subbands.

5) Power Constraints: The signals $\mathbf{x}_{i,r}^{(i)}$ and $\mathbf{x}_{i,r}^{(S)}$ transmitted by RU (i,r) on the private and shared subbands are given as $\mathbf{x}_{i,r}^{(i)} = \hat{\mathbf{x}}_{i,r}^{(i)}$ and $\mathbf{x}_{i,r}^{(S)} = \hat{\mathbf{x}}_{i,r}^{(S)} + \mathbf{r}_{i,r}^{(S)}$, respectively. We impose per-RU transmission power constraints as

$$W_{P,i} p_{i,r}^{(i)}\left(\mathbf{V}, \mathbf{\Omega}\right) + W_S p_{i,r}^{(S)}\left(\mathbf{V}, \mathbf{T}, \mathbf{\Omega}, \mathbf{\Sigma}\right) \le P_{i,r}, \quad (14)$$

for $i \in \mathcal{N}_O$, $r \in \mathcal{N}_R$, where $P_{i,r}$ represents the maximum transmission power allowed for RU (i,r), and the functions $p_{i,r}^{(i)}(\mathbf{V}, \mathbf{\Omega})$ and $p_{i,r}^{(S)}(\mathbf{V}, \mathbf{T}, \mathbf{\Omega}, \mathbf{\Sigma})$ measure the transmission powers per unit bandwidth on the private and shared subbands, respectively, as

$$p_{i,r}^{(i)}\left(\mathbf{V}, \mathbf{\Omega}\right) \triangleq \mathtt{E}\left\|\mathbf{x}_{i,r}^{(i)}\right\|^2 = \left(\sum_{k\in\mathcal{N}_U} \mathrm{tr}\left(\mathbf{K}\left(\mathbf{E}_{i,r}^\dagger \mathbf{V}_{i,k}^{(i)}\right)\right) + \mathrm{tr}\left(\mathbf{\Omega}_{i,r}^{(i)}\right)\right), \quad (15)$$

$$p_{i,r}^{(S)}\left(\mathbf{V}, \mathbf{T}, \mathbf{\Omega}, \mathbf{\Sigma}\right) \triangleq \mathtt{E}\left\|\mathbf{x}_{i,r}^{(S)}\right\|^2 = \begin{pmatrix} \sum_{k\in\mathcal{N}_U} \mathrm{tr}\left(\mathbf{K}\left(\mathbf{E}_{i,r}^\dagger \mathbf{V}_{i,k}^{(S)}\right)\right) + \mathrm{tr}\left(\mathbf{\Omega}_{i,r}^{(S)}\right) \\ + \sum_{k\in\mathcal{N}_U} \mathrm{tr}\left(\mathbf{K}\left(\mathbf{E}_{i,r}^\dagger \mathbf{T}_{i,k}^{(S)}\right)\right) + \mathrm{tr}\left(\mathbf{\Sigma}_{i,r}^{(S)}\right) \end{pmatrix}. \quad (16)$$

C. Decoding at UEs and Achievable Rates

Each UE (i,k) decodes the the submessage $M_{i,k,P}$ transmitted on the private subband based on the received signal $\mathbf{y}_{i,k}^{(i)}$, while treating the interference signals as additive noise. Then, the maximum achievable rate $R_{i,k,P}$ of the submessage $M_{i,k,P}$ can be written as

$$R_{i,k,P} = W_{P,i} I\left(\mathbf{s}_{i,k,P};\, \mathbf{y}_{i,k}^{(i)}\right), \tag{17}$$

where

$$I\left(\mathbf{s}_{i,k,P};\, \mathbf{y}_{i,k}^{(i)}\right) = f_{i,k,P}\left(\mathbf{V}, \mathbf{\Omega}\right) = \Phi\left(\mathbf{K}\left(\mathbf{H}_{i,k}^{i}\mathbf{V}_{i,k}^{(i)}\right), \begin{pmatrix} \sum_{l\in\mathcal{N}_U\setminus\{k\}} \mathbf{K}\left(\mathbf{H}_{i,k}^{i}\mathbf{V}_{i,l}^{(i)}\right) \\ +\mathbf{H}_{i,k}^{i}\mathbf{\Omega}_{i}^{(i)}\mathbf{H}_{i,k}^{i\,\dagger} + \mathbf{I} \end{pmatrix}\right). \tag{18}$$

Here we defined the channel matrix $\mathbf{H}_{i,k}^{j} = [\mathbf{H}_{i,k}^{j,1}\mathbf{H}_{i,k}^{j,2}\cdots \mathbf{H}_{i,k}^{j,N_R}]$ from all the RUs of operator j to UE (i,k), and the matrix $\mathbf{\Omega}_{i}^{(i)} = \mathrm{diag}(\mathbf{\Omega}_{i,1}^{(i)},\ldots,\mathbf{\Omega}_{i,N_R}^{(i)})$.

In a similar manner, we assume that UE (i,k) decodes the submessage $M_{i,k,S}$ sent on the shared subband from the received signal $\mathbf{y}_{i,k}^{(S)}$ by treating the interference signals as noise, so that the maximum achievable rate $R_{i,k,S}$ is given as

$$R_{i,k,S} = W_S I\left(\mathbf{s}_{i,k,S};\, \mathbf{y}_{i,k}^{(S)}\right), \tag{19}$$

with the mutual information $I(\mathbf{s}_{i,k,S};\, \mathbf{y}_{i,k}^{(S)})$ given as

$$I(\mathbf{s}_{i,k,S};\, \mathbf{y}_{i,k}^{(S)}) = f_{i,k,S}\left(\mathbf{V},\mathbf{T},\mathbf{\Omega},\mathbf{\Sigma}\right) = \Phi\left(\mathbf{K}\begin{pmatrix}\mathbf{H}_{i,k}^{i}\mathbf{V}_{i,k}^{(S)} \\ +\mathbf{H}_{i,k}^{\bar{i}}\mathbf{T}_{\bar{i},k}^{(S)}\end{pmatrix}, \begin{pmatrix} \sum_{l\in\mathcal{N}_U\setminus\{k\}} \mathbf{K}\begin{pmatrix}\mathbf{H}_{i,k}^{i}\mathbf{V}_{i,l}^{(S)} \\ +\mathbf{H}_{i,k}^{\bar{i}}\mathbf{T}_{\bar{i},l}^{(S)}\end{pmatrix} \\ +\sum_{l\in\mathcal{N}_U} \mathbf{K}\begin{pmatrix}\mathbf{H}_{i,k}^{i}\mathbf{T}_{i,l}^{(S)} \\ +\mathbf{H}_{i,k}^{\bar{i}}\mathbf{V}_{\bar{i},l}^{(S)}\end{pmatrix} \\ +\mathbf{H}_{i,k}^{i}\left(\mathbf{\Omega}_{i}^{(S)}+\mathbf{\Sigma}_{i}^{(S)}\right)\mathbf{H}_{i,k}^{i\,\dagger} \\ +\mathbf{H}_{i,k}^{\bar{i}}\left(\mathbf{\Omega}_{\bar{i}}^{(S)}+\mathbf{\Sigma}_{\bar{i}}^{(S)}\right)\mathbf{H}_{i,k}^{\bar{i}\,\dagger}+\mathbf{I}\end{pmatrix}\right), \tag{20}$$

where we defined the matrices $\mathbf{\Omega}_{i}^{(S)} = \mathrm{diag}(\mathbf{\Omega}_{i,1}^{(S)},\ldots,\mathbf{\Omega}_{i,N_R}^{(S)})$ and $\mathbf{\Sigma}_{i}^{(S)} = \mathrm{diag}(\mathbf{\Sigma}_{i,1}^{(S)},\ldots,\mathbf{\Sigma}_{i,N_R}^{(S)})$.

D. Privacy Constraints

As discussed, inter-operator cooperation on the shared subband requires the transmission of precoded and quantized signals $\{\mathbf{r}_{\bar{i},r}^{(S)}\}_{r\in\mathcal{N}_R}$ between CP i and CP $\bar{i}$ on the backhaul link. As a result, CP $\bar{i}$ can infer some information about the messages $\{M_{i,k,S}\}_{k\in\mathcal{N}_U}$ intended for the UEs (i,k), $k\in\mathcal{N}_U$, of the operator i. In order to ensure that this leakage of information is limited, one can design both the precoding matrices $\mathbf{T}$ and the quantization covariance matrices $\mathbf{\Sigma}$ under the information-theoretic privacy constraint

$$W_S I\left(\mathbf{s}_{i,k,S};\, \left\{\mathbf{r}_{\bar{i},r}^{(S)}\right\}_{r\in\mathcal{N}_R}\right) \le \Gamma_{\text{privacy}}. \tag{21}$$

In (21), the mutual information $I(\mathbf{s}_{i,k,S};\, \{\mathbf{r}_{\bar{i},r}^{(S)}\}_{r\in\mathcal{N}_R})$ measures the amount of the information that can be inferred about each signal $\mathbf{s}_{i,k,S}$ by the CP $\bar{i}$ of the other operator based on the observation of $\{\mathbf{r}_{\bar{i},r}^{(S)}\}_{r\in\mathcal{N}_R}$. This mutual information can be written as

$$I\left(\mathbf{s}_{i,k,S};\, \left\{\mathbf{r}_{\bar{i},r}^{(S)}\right\}_{r\in\mathcal{N}_R}\right) = \beta_{i,k,S}\left(\mathbf{T},\mathbf{\Sigma}\right) = \Phi\left(\mathbf{K}\left(\mathbf{T}_{\bar{i},k}^{(S)}\right), \sum_{l\in\mathcal{N}_U\setminus\{k\}} \mathbf{K}\left(\mathbf{T}_{\bar{i},l}^{(S)}\right) + \mathbf{\Sigma}_{\bar{i}}^{(S)}\right). \tag{22}$$

The condition (21) imposes that the amount of leaked information does not exceed a predetermined threshold value Γ_{privacy}. This value has a specific operational meaning according to standard information-theoretic results [33, Ch. 4, Problem 33]. In particular, a privacy level of Γ_{privacy} implies that, if a user receives at rate R (bit/s) on shared subband, a bit stream of rate $(R-\Gamma_{\text{privacy}})^+$ can be received securely, while the remaining rate $\min(\Gamma_{\text{privacy}}, R)$ (bit/s) can be eavesdropped by the other operator. Here $[\cdot]^+$ is defined as $[a]^+ = \max\{a,0\}$.

In ensuring the satisfaction of the privacy constraint (21), the quantization noise introduced by the fronthaul quantization plays an important role. In fact, the fronthaul quantization noise is instrumental in masking information about the UE messages at the cost of a more significant degradation of the signals received by the UEs. A more advanced quantization scheme will be considered in Sec. V.

IV. Optimization of Multi-Tenant C-RAN

We aim at jointly optimizing the bandwidth allocation $\mathbf{W}$, the precoding matrices $\{\mathbf{V},\mathbf{T}\}$ and the quantization noise covariance matrices $\{\mathbf{\Omega},\mathbf{\Sigma}\}$, with the goal of maximizing the sum-rate $R_\Sigma \triangleq \sum_{i\in\mathcal{N}_O}\sum_{k\in\mathcal{N}_U}(R_{i,k,P}+R_{i,k,S})$ of all the UEs, under constraints on backhaul and fronthaul capacity, per-RU transmit power and inter-operator privacy levels. The problem can be stated as

$$\underset{\mathbf{V},\mathbf{T},\mathbf{\Omega},\mathbf{\Sigma},\mathbf{W},\mathbf{R}}{\text{maximize}} \quad \sum_{i\in\mathcal{N}_O}\sum_{k\in\mathcal{N}_U}(R_{i,k,P}+R_{i,k,S}) \tag{23a}$$

$$\text{s.t.} \quad R_{i,k,P} \le W_{P,i} f_{i,k,P}\left(\mathbf{V},\mathbf{\Omega}\right), \quad i\in\mathcal{N}_O,\, k\in\mathcal{N}_U, \tag{23b}$$

$$R_{i,k,S} \le W_S f_{i,k,S}\left(\mathbf{V},\mathbf{T},\mathbf{\Omega},\mathbf{\Sigma}\right), \quad i\in\mathcal{N}_O,\, k\in\mathcal{N}_U, \tag{23c}$$

$$\sum_{r\in\mathcal{N}_R} W_S \gamma_{\bar{i},r}^{(S)}\left(\mathbf{T},\mathbf{\Sigma}\right) \le C_{B,i},\ i\in\mathcal{N}_O, \tag{23d}$$

$$\sum_{m\in\{i,S\}} W_{i,m} g_{i,r}^{(m)}\left(\mathbf{V},\mathbf{\Omega}\right) + W_S\gamma_{i,r}^{(S)}\left(\mathbf{T},\mathbf{\Sigma}\right) \le C_{F,i,r},\ i\in\mathcal{N}_O,\, r\in\mathcal{N}_R, \tag{23e}$$

$$W_S \beta_{i,k,S}\left(\mathbf{T},\mathbf{\Sigma}\right) \leq \Gamma_{\text{privacy}},$$
$$i \in \mathcal{N}_O,\, k \in \mathcal{N}_U, \tag{23f}$$
$$W_{P,i} p_{i,r}^{(i)}\left(\mathbf{V},\mathbf{\Omega}\right) + W_S p_{i,r}^{(S)}\left(\mathbf{V},\mathbf{T},\mathbf{\Omega},\mathbf{\Sigma}\right) \leq P_{i,r},\ i \in \mathcal{N}_O,\, r \in \mathcal{N}_R, \tag{23g}$$
$$W_{P,1} + W_{P,2} + W_S = W. \tag{23h}$$

In (23), constraints (23b)–(23c) follow from the achievable rates (17) and (19); (23d)–(23e) are the backhaul and fronthaul capacity constraints (12) and (13); (23f) is the inter-operator privacy constraint (21); (23g) is the per-RU transmit power constraint (14); and (23h) is the sum-bandwidth constraint (3).

Since the problem (23) is non-convex, we adopt a Successive Convex Approximation (SCA) approach to obtain an efficient local optimization algorithm. To this end, we equivalently rewrite the constraints (23b) and (23c) using the epigraph form as

$$\log R_{i,k,P} \leq \log W_{P,i} + \log t_{f,i,k,P},\ i \in \mathcal{N}_O,\, k \in \mathcal{N}_U, \tag{24}$$

$$t_{f,i,k,P} \leq f_{i,k,P}\left(\mathbf{V},\mathbf{\Omega}\right),\ i \in \mathcal{N}_O,\, k \in \mathcal{N}_U, \tag{25}$$

and

$$\log R_{i,k,S} \leq \log W_S + \log t_{f,i,k,S},\ i \in \mathcal{N}_O,\, k \in \mathcal{N}_U, \tag{26}$$

$$t_{f,i,k,S} \leq f_{i,k,S}\left(\mathbf{V},\mathbf{T},\mathbf{\Omega},\mathbf{\Sigma}\right)\ i \in \mathcal{N}_O,\, k \in \mathcal{N}_U, \tag{27}$$

respectively. We note that the conditions (24) and (26) are difference-of-convex (DC) constraints (see, e.g., [11], [13]), and that the conditions (25) and (27) can be converted into DC constraints by expressing them with respect to the variables $\tilde{\mathbf{V}}_{i,k}^{(i)} = \mathbf{V}_{i,k}^{(i)}\mathbf{V}_{i,k}^{(i)\dagger}$ and $\tilde{\mathbf{U}}_{i,k}^{(S)} = \mathbf{U}_{i,k}^{(S)}\mathbf{U}_{i,k}^{(S)\dagger}$ with $\mathbf{U}_{i,k}^{(S)} = [\mathbf{V}_{i,k}^{(S)\dagger}\ \mathbf{T}_{i,k}^{(S)\dagger}]^{\dagger}$. Similarly, the other non-convex constraints (23e)–(23g) can also be transformed into DC conditions by relaxing the non-convex rank constraints $\text{rank}(\tilde{\mathbf{V}}_{i,k}^{(i)}) \leq d_{i,k,P}$ and $\text{rank}(\tilde{\mathbf{U}}_{i,k}^{(S)}) \leq d_{i,k,S}$. As a result of these manipulations, we finally obtain the DC problem (31) reported in Appendix.

We tackle the obtained DC problem by deriving an iterative algorithm based on the standard concave convex procedure (CCCP) approach [11], [13]. The detailed algorithm is described in Algorithm 1. In our simulations, we used the CVX software [34] to solve the convex problem (32) (see Appendix) at Step 2. The complexity of Algorithm 1 is given as the number of iterations multiplied by the complexity of solving each convex program (32) shown in Appendix. The latter can be seen to be polynomial in the problem size, which is given as $\mathcal{O}(N_O n_R^2 (N_U + N_R))$ assuming $n_{R,i,r} = n_R$ for all $i \in \mathcal{N}_O$ and $r \in \mathcal{N}_R$, by the use of interior point algorithms (see [35, Ch. 1 and Ch. 11]). For the number of iterations, we provide numerical evidence of the fast convergence of the proposed algorithm in Sec. VI.

After the convergence of the algorithm, we need to project the variables $\tilde{\mathbf{V}}_{i,k}^{(i)\prime\prime}$ and $\tilde{\mathbf{U}}_{i,k}^{(S)\prime\prime}$ onto the spaces of limited-rank matrices satisfying $\text{rank}(\tilde{\mathbf{V}}_{i,k}^{(i)}) \leq d_{i,k,P}$ and $\text{rank}(\tilde{\mathbf{U}}_{i,k}^{(S)}) \leq d_{i,k,S}$, respectively. Without claim of optimality, we use the standard approach of obtaining the variables $\tilde{\mathbf{V}}_{i,k}^{(i)}$ and $\tilde{\mathbf{U}}_{i,k}^{(S)}$ by including the $d_{i,k,P}$ and $d_{i,k,S}$ leading eigenvectors of the matrices $\tilde{\mathbf{V}}_{i,k}^{(i)\prime\prime}$ and $\tilde{\mathbf{U}}_{i,k}^{(S)\prime\prime}$, respectively, as columns.

Algorithm 1: CCCP Algorithm For Problem (31).

1. Initialize the variables $\tilde{\mathbf{V}}'$, $\tilde{\mathbf{U}}'$, $\mathbf{\Omega}'$, $\mathbf{\Sigma}'$, $\mathbf{W}'$ and $\mathbf{R}'$ to arbitrary feasible values that satisfy the constraints of problem (31).
2. Update the variables $\tilde{\mathbf{V}}''$, $\tilde{\mathbf{U}}''$, $\mathbf{\Omega}''$, $\mathbf{\Sigma}''$, $\mathbf{W}''$ and $\mathbf{R}''$ as a solution of the convex problem (32) in Appendix.
3. Stop if a convergence criterion is satisfied. Otherwise, set $\tilde{\mathbf{V}}' \leftarrow \tilde{\mathbf{V}}''$, $\tilde{\mathbf{U}}' \leftarrow \tilde{\mathbf{U}}''$, $\mathbf{\Omega}' \leftarrow \mathbf{\Omega}''$, $\mathbf{\Sigma}' \leftarrow \mathbf{\Sigma}''$, $\mathbf{W}' \leftarrow \mathbf{W}''$ and $\mathbf{R}' \leftarrow \mathbf{R}''$ and go back to Step 2.

V. Multivariate Compression

In this section, we propose a novel quantization approach for inter-CP communication that aims at controlling the trade-off between the distortion at the UEs and inter-operator privacy. The approach is based on multivariate compression, first studied for single-tenant systems in [11], [14]. To highlight the idea, we focus on the case of single RU per operator, i.e., $N_R = 1$, but extensions follow in the same way, albeit at the cost of a more cumbersome notation.

The key idea is for each CP i to jointly quantize the precoded signals to be transmitted by the tenants' RUs. In so doing, one can better control the impact of the quantization noise on the UEs' decoders, while still ensuring a given level of privacy with respect to CP $\bar{i}$.

Mathematically, CP i produces the linearly precoded signals $\tilde{\mathbf{x}}_{i,1}^{(S)}$ and $\tilde{\mathbf{r}}_{\bar{i},1}^{(S)}$ according to (5) and (6), respectively, and obtains the quantized signals $\hat{\mathbf{x}}_{i,1}^{(S)} = \tilde{\mathbf{x}}_{i,1}^{(S)} + \mathbf{q}_{i,1}^{(S)}$ and $\mathbf{r}_{\bar{i},1}^{(S)} = \tilde{\mathbf{r}}_{\bar{i},1}^{(S)} + \mathbf{e}_{\bar{i},1}^{(S)}$ that are transferred to RUs $(i,1)$ and $(\bar{i},1)$, respectively. With multivariate compression of the precoded signals $\tilde{\mathbf{x}}_{i,1}^{(S)}$ and $\tilde{\mathbf{r}}_{\bar{i},1}^{(S)}$, CP i can ensure that the quantization noise signals $\mathbf{q}_{i,1}^{(S)}$ and $\mathbf{e}_{\bar{i},1}^{(S)}$ have a correlation matrix $\mathbf{\Theta}_i^{(S)} = \mathtt{E}[\mathbf{q}_{i,1}^{(S)}\mathbf{e}_{\bar{i},1}^{(S)\dagger}]$. As a result, the effective quantization noise signal that affects the received signal $\mathbf{y}_{j,k}^{(S)}$ of UE (j,k) on the shared subband is given as $\tilde{\mathbf{q}}_{j,k}^{(S)} = \mathbf{H}_{j,k}^{i}\mathbf{q}_{i,1}^{(S)} + \mathbf{H}_{j,k}^{\bar{i}}\mathbf{e}_{\bar{i},1}^{(S)}$, whose covariance matrix depends on the correlation matrix $\mathbf{\Theta}_i^{(S)}$ as

$$\mathtt{E}\left[\tilde{\mathbf{q}}_{j,k}^{(S)}\tilde{\mathbf{q}}_{j,k}^{(S)\dagger}\right] = \mathbf{G}_{j,k}^{i}\mathbf{\Lambda}_i\mathbf{G}_{j,k}^{i\dagger}, \tag{28}$$

where the matrix $\mathbf{\Lambda}_i$ represents the covariance matrix of the stacked quantization noise signals $[\mathbf{q}_{i,1}^{(S)\dagger}\ \mathbf{e}_{\bar{i},1}^{(S)\dagger}]^{\dagger}$ as

$$\mathbf{\Lambda}_i = \mathtt{E}\left[\begin{bmatrix}\mathbf{q}_{i,1}^{(S)}\\ \mathbf{e}_{\bar{i},1}^{(S)}\end{bmatrix}\begin{bmatrix}\mathbf{q}_{i,1}^{(S)\dagger}\ \mathbf{e}_{\bar{i},1}^{(S)\dagger}\end{bmatrix}\right] = \begin{bmatrix}\mathbf{\Omega}_{i,1}^{(S)} & \mathbf{\Theta}_i^{(S)}\\ \mathbf{\Theta}_i^{(S)\dagger} & \mathbf{\Sigma}_{\bar{i},1}^{(S)}\end{bmatrix} \succeq \mathbf{0}. \tag{29}$$

Designing $\mathbf{\Theta}_i^{(S)}$ hence allows us to control the effective noise observed by the UE, while also affecting the inter-operator privacy constraint (21).

For the optimization under multivariate compression, it was shown in [32, Ch. 9] that correlating the quantization noise sig-

nals imposes the following additional constraint on the variables $t_{g,i,1,S}$ and $t_{\gamma,\bar{i},r,S}$ in the DC problem (31) detailed in Appendix:

$$h\left(\hat{\mathbf{x}}_{i,1}^{(S)}\right)+h\left(\mathbf{r}_{\bar{i},1}^{(S)}\right)-h\left(\hat{\mathbf{x}}_{i,1}^{(S)},\mathbf{r}_{\bar{i},1}^{(S)}|\tilde{\mathbf{x}}_{i,1}^{(S)},\tilde{\mathbf{r}}_{\bar{i},1}^{(S)}\right)$$
$$=\log_2\det\left(\sum_{k\in\mathcal{N}_U}\tilde{\mathbf{E}}_{i,1}^{\dagger}\tilde{\mathbf{U}}_{i,k}^{(S)}\tilde{\mathbf{E}}_{i,1}+\mathbf{\Omega}_{i,1}^{(S)}\right)$$
$$+\log_2\det\left(\sum_{k\in\mathcal{N}_U}\bar{\mathbf{E}}_{i,1}^{\dagger}\tilde{\mathbf{U}}_{i,k}^{(S)}\bar{\mathbf{E}}_{i,1}+\mathbf{\Sigma}_{\bar{i},1}^{(S)}\right)$$
$$-\log_2\det\left(\mathbf{\Lambda}_i\right)\leq t_{g,i,1,S}+t_{\gamma,\bar{i},r,S}. \tag{30}$$

The optimization under multivariate quantization is stated as the problem (31) in Appendix with the constraint (30) added. We can handle the problem following Algorithm 1 since the added condition is a DC constraint.

VI. Numerical Results

In this section, we present numerical results that validate the performance of multi-tenant C-RAN systems with spectrum pooling in the presence of the proposed optimization and quantization strategies. We assume that the positions of the RUs and UEs are uniformly distributed within a circular area of radius 100 m. For given positions of the RUs and the UEs, the channel matrix $\mathbf{H}_{i,k}^{j,r}$ from RU (j,r) to UE (i,k) is modeled as $\mathbf{H}_{i,k}^{j,r}=\sqrt{\rho_{i,k}^{j,r}}\tilde{\mathbf{H}}_{i,k}^{j,r}$, where $\rho_{i,k}^{j,r}=1/(1+(D_{i,k}^{j,r}/D_0)^{\alpha})$ represents the path-loss, $D_{i,k}^{j,r}$ is the distance between the RU (j,r) to UE (i,k), and the elements of $\tilde{\mathbf{H}}_{i,k}^{j,r}$ are independent and identically distributed (i.i.d.) as $\mathcal{CN}(0,1)$. In the simulation, we set $\alpha=3$ and $D_0=50$ m. Except for Fig. 9, we focus on the point-to-point compression strategy studied in Sec. III and Sec. IV.

To validate the effectiveness of the proposed designs, we compare the following three schemes:

- Spectrum pooling with optimized bandwidth allocation $W_{P,1}$, $W_{P,2}$ and W_S;
- Spectrum pooling with equal bandwidth allocation $W_{P,1}=W_{P,2}=W_S=W/3$;
- No spectrum pooling with equal bandwidth allocation $W_{P,1}=W_{P,2}=W/2$ and $W_S=0$.

The first approach adopts the proposed optimization algorithm (see Algorithm 1) discussed in Sec. IV. Instead, the other two baseline approaches are obtained by using the proposed algorithm with the added linear equality constraints $W_{P,1}=W_{P,2}=W_S=W/3$, or $W_{P,1}=W_{P,2}=W/2$ and $W_S=0$, respectively. Except for the last scheme with no spectrum pooling, all schemes exhibit a trade-off between the achievable sum-rate and the guaranteed privacy level Γ_{privacy}. A smaller Γ_{privacy}, i.e., a stricter privacy constraint, generally entails a smaller sum-rate, and vice versa for a larger Γ_{privacy}. To quantify this effect, we define the per-UE secrecy rate $R_{U,\text{sec}}$ as $R_{U,\text{sec}}=[R_U-\Gamma_{\text{privacy}}]^+$, where R_U is the average per-UE achievable rate. The rate R_U is given by the total sum-rate R_Σ divided by the number of total UEs, i.e., $R_U=R_\Sigma/(2N_U)$. Following the discussion in Sec. III-D, the quantity $R_{U,\text{sec}}$ measures the rate at which information is transmitted privately to each UE. In contrast, R_U represents the overall transmission rate, including both secure and insecure data streams.

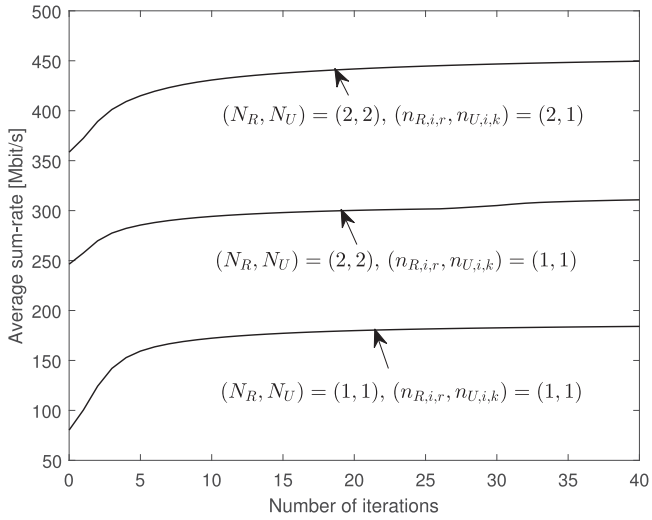

(a) 0 dB SNR

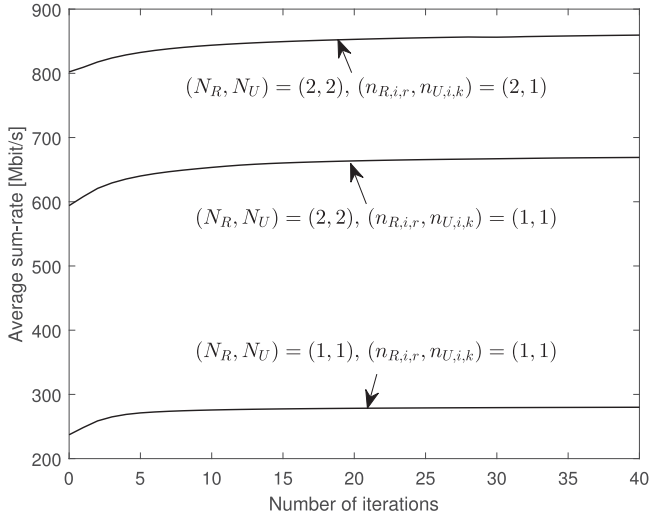

(b) 10 dB SNR

Fig. 4. Average per-UE rate versus the number of iterations ($N_R=N_U\in\{1,2\}$, $n_{R,i,r}\in\{1,2\}$, $n_{U,i,k}=1$, $C_{B,i}=1$ Gbit/s, $C_{F,i,r}=500$ Mbit/s, $W=100$ MHz, $\Gamma_{\text{privacy}}=200$ Mbit/s and 0, 10 dB SNRs).

In Fig. 4, we elaborate on the convergence speed of Algorithm 1 by plotting the average per-UE rate versus the number of iterations for $N_R=N_U\in\{1,2\}$, $n_{R,i,r}\in\{1,2\}$, $n_{U,i,k}=1$, $C_{B,i}=1$ Gbit/s, $C_{F,i,r}=500$ Mbit/s, $W=100$ MHz, $\Gamma_{\text{privacy}}=200$ Mbit/s and 0, 10 dB SNRs. The figure suggests, along with our extensive experiments, that the proposed algorithm converges with a few tens of iterations.

Fig. 5 plots the average per-UE rate R_U versus the average per-UE secrecy rate $R_{U,\text{sec}}$ for a multi-tenant C-RAN with $N_R=N_U=2, n_{R,i,r}=n_{U,i,k}=1, C_{B,i}=1$ Gbit/s, $C_{F,i,r}=500$ Mbit/s, $W=100$ MHz and 10, 15 and 20 dB signal-to-noise ratios (SNRs). The curves are obtained by varying the

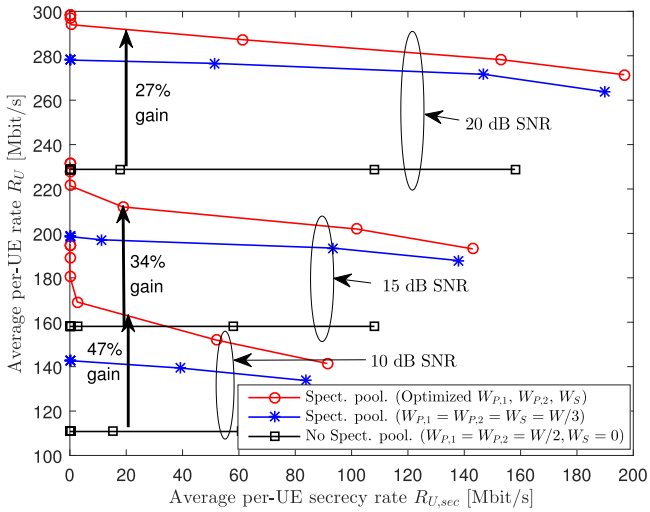

Fig. 5. Average per-UE rate R_U versus average per-UE secrecy rate $R_{U,\text{sec}}$ ($N_R = N_U = 2$, $n_{R,i,r} = n_{U,i,k} = 1$, $C_{B,i} = 1$ Gbit/s, $C_{F,i,r} = 500$ Mbit/s and $W = 100$ MHz).

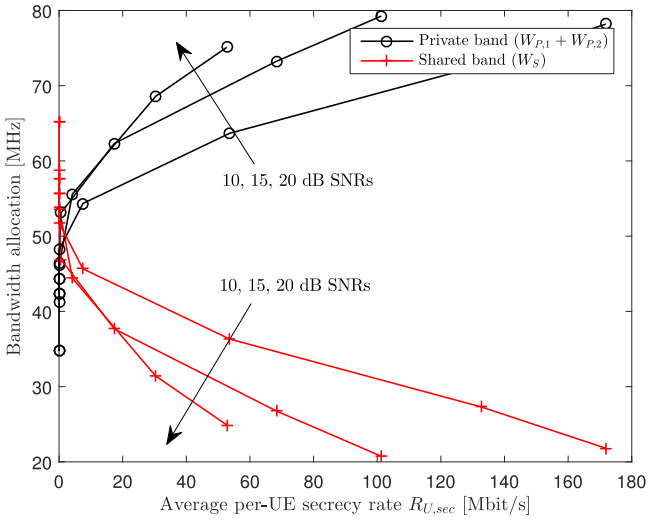

Fig. 6. Bandwidth allocation versus average per-UE secrecy rate $R_{U,\text{sec}}$ ($N_R = N_U = 1$, $n_{R,i,r} = n_{U,i,k} = 1$, $C_{B,i} = 1$ Gbit/s, $C_{F,i,r} = 500$ Mbit/s and $W = 100$ MHz).

privacy threshold levels ranging from 5 Mbit/s to 60 Mbit/s in the constraints (23f). In the figure, the multi-tenant C-RAN system with the proposed optimization achieves a significantly improved rate-privacy trade-off as compared to the other two strategies with no spectrum pooling or uniform spectrum allocation. The gain becomes more significant at lower SNR and larger privacy levels, since the impact of inter-operator cooperation in the shared subband is more pronounced in this regime. As an example, in order to guarantee the per-UE secrecy rate of 20 Mbit/s, the proposed multi-tenant C-RAN system achieves a gain of about 47% gain in terms of per-UE rates at 10 dB SNR with respect to the traditional C-RAN system without spectrum pooling.

Fig. 6 plots the average bandwidth allocation between the private and shared subbands versus the average per-UE secrecy rate $R_{U,\text{sec}}$ for the set-up considered in Fig. 5, but with $N_R = N_U = 1$. Consistently with the discussion above, as the SNR

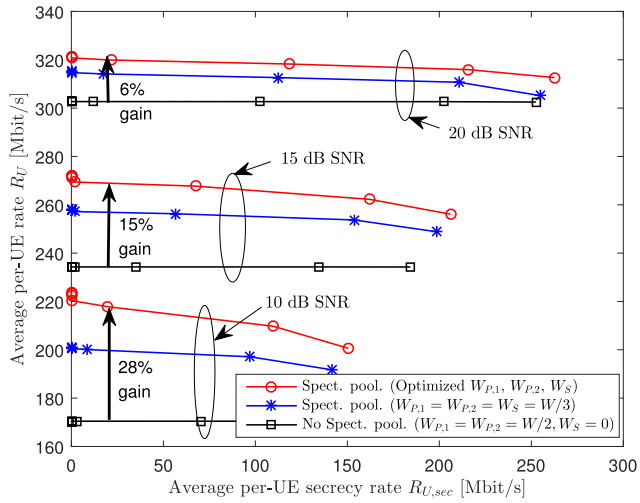

Fig. 7. Average per-UE rate R_U versus average per-UE secrecy rate $R_{U,\text{sec}}$ ($N_R = N_U = 2, n_{R,i,r} = 2, n_{U,i,k} = 1, C_{B,i} = 1$ Gbit/s, $C_{F,i,r} = 500$ Mbit/s and $W = 100$ MHz).

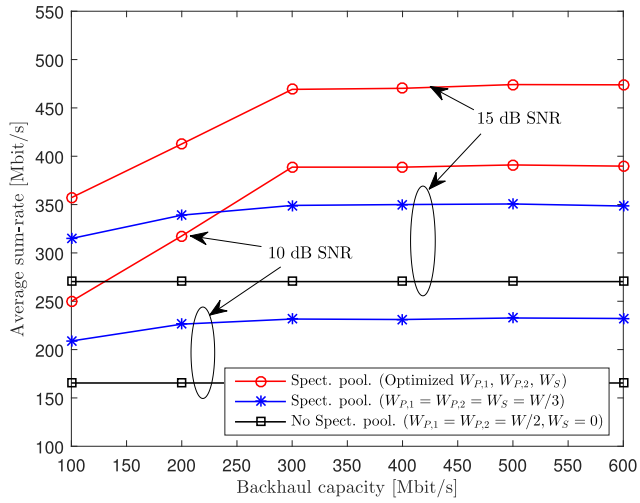

(a)

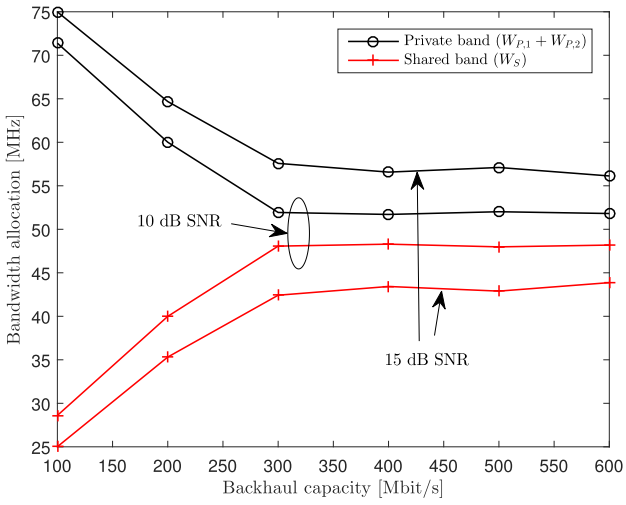

(b)

Fig. 8. (a) Average sum-rate R_Σ. (b) Bandwidth allocation versus the backhaul capacity $C_{F,i}$ ($N_R = N_U = 1$, $n_{R,i,r} = n_{U,i,k} = 1$, $C_{F,i,r} = 500$ Mbit/s, $W = 100$ MHz, $\Gamma_{\text{privacy}} = 300$ Mbit/s and 15, 20 dB SNRs).

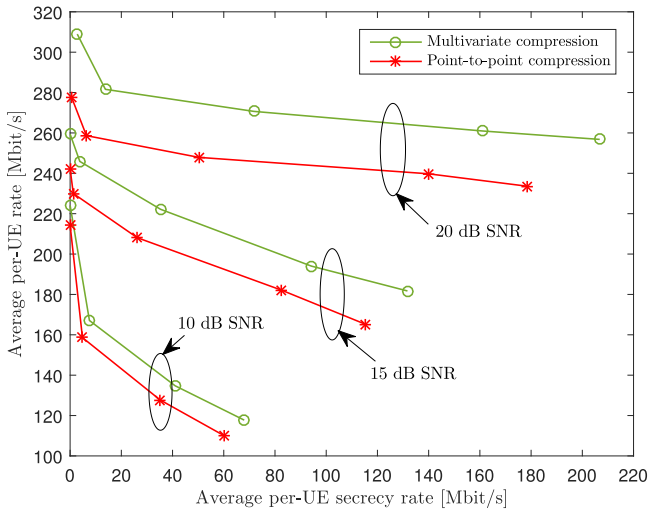

(a)

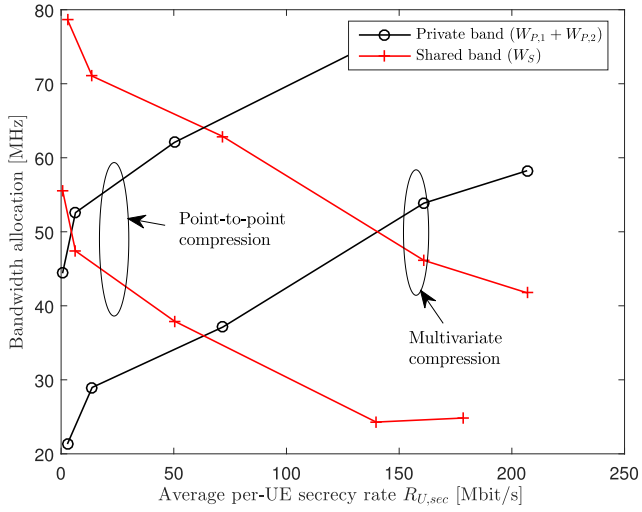

(b)

Fig. 9. (a) Average per-UE rate R_U. (b) Bandwidth allocation versus average per-UE secrecy rate $R_{U,\text{sec}}$ ($N_R = N_U = 1, n_{R,i,r} = n_{U,i,k} = 1, C_{B,i} = 1$ Gbit/s, $C_{F,i,r} = 500$ Mbit/s and $W = 100$ MHz).

decreases, it is seen that more spectrum resources are allocated to the shared subband in order to leverage the opportunity of inter-operator cooperation.

In Fig. 7, we elaborate on the effect of the number of antennas. To this end, we show the average per-UE rate R_U versus the average per-UE secrecy rate $R_{U,\text{sec}}$ for a multi-tenant C-RAN with the same set-up as in Fig. 5 except for $n_{R,i,r} = 2$ instead of $n_{R,i,r} = 1$. We can see that, compared to the single-antenna case, all the three schemes become more robust to the privacy constraint with an increased number of RU and UE antennas. This is due to the additional degrees of freedom in the precoding design that is afforded by the larger number of antennas.

In Fig. 8, we plot the average sum-rate and the optimized bandwidth allocation versus the backhaul capacity $C_{B,i}$ for a multi-tenant C-RAN with $N_R = N_U = 1, n_{R,i,r} = n_{U,i,k} = 1$, $C_{F,i,r} = 500$ Mbit/s, $W = 100$ MHz, $\Gamma_{\text{privacy}} = 300$ Mbit/s and 10, 15 dB SNRs. The figure shows that, as the backhaul capacity increases, a larger bandwidth is allocated to the shared subband, since the CPs can exchange better descriptions of the precoded signals through the backhaul links of larger capacity. However, if the backhaul capacity exceeds a threshold value, both the sum-rate performance and the optimized bandwidth saturate, since the presence of inter-operator privacy constraints limits the opportunities for inter-operator cooperation.

We now study the impact of correlating the quantization noise signals across the RUs of operators by means of the multivariate compression strategy proposed in Sec. V. In Fig. 9(a), we plot the average per-UE rate R_U versus the average per-UE secrecy rate $R_{U,\text{sec}}$ for the same multi-tenant C-RAN set-up considered in Fig. 6 assuming spectrum pooling with optimized bandwidths $\{W_{P,1}, W_{P,2}, W_S\}$. We observe that multivariate compression is instrumental in improving the trade-off between inter-operator cooperation and privacy. The accrued performance gain increases with the SNR, since the performance degradation due to quantization is masked by the additive noise when the SNR is small. Fig. 9(b) plots the optimized bandwidth allocation versus the average per-UE secrecy rate $R_{U,\text{sec}}$ for a 20 dB SNR. The figure suggests that, with multivariate compression, it is desirable to allocate more bandwidth to the shared subband, given the added benefits of inter-operator cooperation in the presence of multivariate compression.

VII. Conclusion

In this work, we have studied the design of multi-tenant C-RAN systems with spectrum pooling under inter-operator privacy constraints. Assuming the standard C-RAN operation with quantized baseband signals, we first considered the standard point-to-point compression strategy, and then proposed a novel multivariate compression to achieve a better trade-off between the inter-operator cooperation and privacy. For both cases, we tackled the joint optimization of the bandwidth allocation among the private and shared subbands and of the precoding and fronthaul/backhaul compression strategies while satisfying constraints on fronthaul and backhaul capacity, per-RU transmit power and inter-operator privacy levels. To tackle the non-convex optimization problems, we converted the problems into DC problems with rank relaxation and derived iterative algorithms based on the standard CCCP. We provided extensive numerical results to validate the effectiveness of the multi-tenant C-RAN system with the proposed optimization algorithm and multivariate compression. From the numerical results, we can conclude that the gain of optimized pooling is more significant for lower SNR levels and smaller number of RU and UE antennas, as long as the privacy constraint is not too strict. Furthermore, multivariate compression generally increases the gain of spectrum pooling. These results confirm the intuition that spectrum pooling is useful in improving the performance of networks with individually limited resources, e.g., limited SNR and number of antennas, provided that inter-operator privacy constraints are not excessively constraining. We note that, with standard multicarrier transmission, the design problem under study would include joint power, fronthaul and secrecy constraints on the optimization variables across all subcarriers. The

resulting problem can be dealt with by using a standard dual decomposition approach [36] by leveraging the approach proposed in this paper. Among open problems, we mention the extension of the design and analysis to models with RAN sharing at the level of RUs; the consideration of hierarchical fog architectures; and the investigation of the effect of noisy or delayed CSI at the spectrum pooling server [26], [27].

APPENDIX

By relaxing the non-convex rank constraints $\text{rank}(\tilde{\mathbf{V}}_{i,k}^{(i)}) \leq d_{i,k,P}$ and $\text{rank}(\tilde{\mathbf{U}}_{i,k}^{(S)}) \leq d_{i,k,S}$ explained in Sec. IV, the problem (23) can be converted into the DC problem

$$\begin{aligned}
\underset{\substack{\tilde{\mathbf{V}},\tilde{\mathbf{U}},\boldsymbol{\Omega},\boldsymbol{\Sigma},\mathbf{W},\\ \mathbf{R},\mathbf{t},\tilde{\mathbf{g}},\tilde{\boldsymbol{\gamma}},\tilde{\mathbf{p}}}}{\text{maximize}} \quad & \sum_{i\in\mathcal{N}_O}\sum_{k\in\mathcal{N}_U}(R_{i,k,P}+R_{i,k,S}) \\
\text{s.t.} \quad & \log R_{i,k,P} \leq \log W_{P,i} + \log t_{f,i,k,P},\ i\in\mathcal{N}_O, k\in\mathcal{N}_U, \\
& t_{f,i,k,P} \leq f_{i,k,P}\left(\tilde{\mathbf{V}},\boldsymbol{\Omega}\right), i\in\mathcal{N}_O, k\in\mathcal{N}_U, \\
& \log R_{i,k,S} \leq \log W_S + \log t_{f,i,k,S}, i\in\mathcal{N}_O, k\in\mathcal{N}_U, \\
& t_{f,i,k,S} \leq f_{i,k,S}\left(\tilde{\mathbf{V}},\tilde{\mathbf{U}},\boldsymbol{\Omega},\boldsymbol{\Sigma}\right), i\in\mathcal{N}_O, k\in\mathcal{N}_U, \\
& \tilde{g}_{i,r}^{(i)} + \tilde{g}_{i,r}^{(S)} + \tilde{\gamma}_{i,r}^{(S)} \leq C_{F,i,r}, i\in\mathcal{N}_O, r\in\mathcal{N}_R, \\
& \log W_{i,m} + \log t_{g,i,r,m} \leq \log \tilde{g}_{i,r}^{(m)}, \\
& \qquad i\in\mathcal{N}_O,\ r\in\mathcal{N}_R,\ m\in\{i,S\}, \\
& g_{i,r}^{(i)}\left(\tilde{\mathbf{V}},\boldsymbol{\Omega}\right) \leq t_{g,i,r,i},\ i\in\mathcal{N}_O,\ r\in\mathcal{N}_R, \\
& g_{i,r}^{(S)}\left(\tilde{\mathbf{U}},\boldsymbol{\Omega}\right) \leq t_{g,i,r,S},\ i\in\mathcal{N}_O,\ r\in\mathcal{N}_R, \\
& \log W_S + \log t_{\gamma,i,r,S} \leq \log \tilde{\gamma}_{i,r}^{(S)}, \\
& \qquad i\in\mathcal{N}_O,\ r\in\mathcal{N}_R, \\
& \gamma_{i,r}^{(S)}\left(\tilde{\mathbf{U}},\boldsymbol{\Sigma}\right) \leq t_{\gamma,i,r,S},\ i\in\mathcal{N}_O,\ r\in\mathcal{N}_R, \\
& \sum_{r\in\mathcal{N}_R}\tilde{\gamma}_{i,r}^{(S)} \leq C_{B,i},\ i\in\mathcal{N}_O, \\
& \log W_S + \log t_{\beta,i,k,S} \leq \log\Gamma_{\text{privacy}}, i\in\mathcal{N}_O, k\in\mathcal{N}_U, \\
& \beta_{i,k,S}\left(\tilde{\mathbf{U}},\boldsymbol{\Sigma}\right) \leq t_{\beta,i,k,S},\ i\in\mathcal{N}_O, k\in\mathcal{N}_U, \\
& \tilde{p}_{i,r}^{(i)} + \tilde{p}_{i,r}^{(S)} \leq P_{i,r},\ i\in\mathcal{N}_O,\ r\in\mathcal{N}_R, \\
& \log W_{i,m} + \log t_{p,i,r,m} \leq \log \tilde{p}_{i,r}^{(m)}, \\
& \qquad i\in\mathcal{N}_O,\ r\in\mathcal{N}_R,\ m\in\{i,S\}, \\
& p_{i,r}^{(m)}\left(\tilde{\mathbf{V}},\tilde{\mathbf{U}},\boldsymbol{\Omega},\boldsymbol{\Sigma}\right) \leq t_{p,i,r,m}, \\
& \qquad i\in\mathcal{N}_O,\ r\in\mathcal{N}_R,\ m\in\{i,S\}, \\
& W_{P,1} + W_{P,2} + W_S = W. \qquad (31)
\end{aligned}$$

Furthermore, at Step 2 in Algorithm 1, the CCCP approach solves the convex problem obtained by linearizing the terms that induce non-convexity of problem (31). This can be written as

$$\begin{aligned}
\underset{\substack{\tilde{\mathbf{V}},\tilde{\mathbf{U}},\boldsymbol{\Omega},\boldsymbol{\Sigma},\mathbf{W},\\ \mathbf{R},\mathbf{t},\tilde{\mathbf{g}},\tilde{\boldsymbol{\gamma}},\tilde{\mathbf{p}}}}{\text{maximize}} \quad & \sum_{i\in\mathcal{N}_O}\sum_{k\in\mathcal{N}_U}(R_{i,k,P}+R_{i,k,S}) \\
\text{s.t.} \quad & \varphi\left(R_{i,k,P}, R'_{i,k,P}\right) \leq \log W_{P,i} + \log t_{f,i,k,P}, \\
& \qquad i\in\mathcal{N}_O,\ k\in\mathcal{N}_U, \\
& t_{f,i,k,P} \leq \hat{f}_{i,k,P}\left(\tilde{\mathbf{V}},\boldsymbol{\Omega},\tilde{\mathbf{V}}',\boldsymbol{\Omega}'\right), i\in\mathcal{N}_O,\ k\in\mathcal{N}_U, \\
& \varphi\left(R_{i,k,S}, R'_{i,k,S}\right) \leq \log W_S + \log t_{f,i,k,S}, \\
& \qquad i\in\mathcal{N}_O,\ k\in\mathcal{N}_U, \\
& t_{f,i,k,S} \leq \hat{f}_{i,k,S}\left(\tilde{\mathbf{V}},\tilde{\mathbf{U}},\boldsymbol{\Omega},\boldsymbol{\Sigma},\tilde{\mathbf{V}}',\tilde{\mathbf{U}}',\boldsymbol{\Omega}',\boldsymbol{\Sigma}'\right), \\
& \qquad i\in\mathcal{N}_O,\ k\in\mathcal{N}_U, \\
& \tilde{g}_{i,r}^{(i)} + \tilde{g}_{i,r}^{(S)} + \tilde{\gamma}_{i,r}^{(S)} \leq C_{F,i,r},\ i\in\mathcal{N}_O, r\in\mathcal{N}_R, \\
& \varphi\left(W_{i,m}, W'_{i,m}\right) + \varphi\left(t_{g,i,r,m}, t'_{g,i,r,m}\right) \leq \log \tilde{g}_{i,r}^{(m)}, \\
& \qquad i\in\mathcal{N}_O,\ r\in\mathcal{N}_R,\ m\in\{i,S\}, \\
& \hat{g}_{i,r}^{(i)}\left(\tilde{\mathbf{V}},\boldsymbol{\Omega},\tilde{\mathbf{V}}',\boldsymbol{\Omega}'\right) \leq t_{g,i,r,i},\ i\in\mathcal{N}_O,\ r\in\mathcal{N}_R, \\
& \hat{g}_{i,r}^{(S)}\left(\tilde{\mathbf{U}},\boldsymbol{\Omega},\tilde{\mathbf{U}}',\boldsymbol{\Omega}'\right) \leq t_{g,i,r,S},\ i\in\mathcal{N}_O,\ r\in\mathcal{N}_R, \\
& \varphi\left(W_S, W'_S\right) + \varphi\left(t_{\gamma,i,r,S}, t'_{\gamma,i,r,S}\right) \leq \log \tilde{\gamma}_{i,r}^{(S)}, \\
& \qquad i\in\mathcal{N}_O,\ r\in\mathcal{N}_R, \\
& \hat{\gamma}_{i,r}^{(S)}\left(\tilde{\mathbf{U}},\boldsymbol{\Sigma},\tilde{\mathbf{U}}',\boldsymbol{\Sigma}'\right) \leq t_{\gamma,i,r,S},\ i\in\mathcal{N}_O,\ r\in\mathcal{N}_R, \\
& \sum_{r\in\mathcal{N}_R}\tilde{\gamma}_{i,r}^{(S)} \leq C_{B,i},\ i\in\mathcal{N}_O, \\
& \varphi\left(W_S, W'_S\right) + \varphi\left(t_{\beta,i,k,S}, t'_{\beta,i,k,S}\right) \\
& \qquad \leq \log\Gamma_{\text{privacy}},\ i\in\mathcal{N}_O,\ k\in\mathcal{N}_U, \\
& \hat{\beta}_{i,k,S}\left(\tilde{\mathbf{U}},\boldsymbol{\Sigma},\tilde{\mathbf{U}}',\boldsymbol{\Sigma}'\right) \leq t_{\beta,i,k,S}, i\in\mathcal{N}_O,\ k\in\mathcal{N}_U, \\
& \tilde{p}_{i,r}^{(i)} + \tilde{p}_{i,r}^{(S)} \leq P_{i,r},\ i\in\mathcal{N}_O,\ r\in\mathcal{N}_R, \\
& \varphi\left(W_{i,m}, W'_{i,m}\right) + \varphi\left(t_{p,i,r,m}, t'_{p,i,r,m}\right) \\
& \leq \log \tilde{p}_{i,r}^{(m)},\ i\in\mathcal{N}_O,\ r\in\mathcal{N}_R,\ m\in\{i,S\}, \\
& p_{i,r}^{(m)}\left(\tilde{\mathbf{V}},\tilde{\mathbf{U}},\boldsymbol{\Omega},\boldsymbol{\Sigma}\right) \leq t_{p,i,r,m}, \\
& \qquad i\in\mathcal{N}_O,\ r\in\mathcal{N}_R,\ m\in\{i,S\}, \\
& W_{P,1} + W_{P,2} + W_S = W, \qquad (32)
\end{aligned}$$

where we defined the functions

$$\begin{aligned}
& \hat{f}_{i,k,P}\left(\tilde{\mathbf{V}},\boldsymbol{\Omega},\tilde{\mathbf{V}}',\boldsymbol{\Omega}'\right) \\
& = \log_2\det\left(\sum_{l\in\mathcal{N}_U}\mathbf{H}_{i,k}^{i}\tilde{\mathbf{V}}_{i,l}^{(i)}\mathbf{H}_{i,k}^{i\dagger} + \mathbf{H}_{i,k}^{i}\boldsymbol{\Omega}_i^{(i)}\mathbf{H}_{i,k}^{i\,\dagger} + \mathbf{I}\right) \\
& - \frac{1}{\ln 2}\varphi\left(\begin{matrix}\sum_{l\in\mathcal{N}_U\setminus\{k\}}\mathbf{H}_{i,k}^{i}\tilde{\mathbf{V}}_{i,l}^{(i)}\mathbf{H}_{i,k}^{i\dagger} + \mathbf{H}_{i,k}^{i}\boldsymbol{\Omega}_i^{(i)}\mathbf{H}_{i,k}^{i\,\dagger} + \mathbf{I}, \\ \sum_{l\in\mathcal{N}_U\setminus\{k\}}\mathbf{H}_{i,k}^{i}\tilde{\mathbf{V}}_{i,l}^{(i)\prime}\mathbf{H}_{i,k}^{i\dagger} + \mathbf{H}_{i,k}^{i}\boldsymbol{\Omega}_i^{(i)\prime}\mathbf{H}_{i,k}^{i\,\dagger} + \mathbf{I}\end{matrix}\right),
\end{aligned}$$

$$\hat{f}_{i,k,S}\left(\tilde{\mathbf{V}},\tilde{\mathbf{U}},\mathbf{\Omega},\mathbf{\Sigma},\tilde{\mathbf{V}}',\tilde{\mathbf{U}}',\mathbf{\Omega}',\mathbf{\Sigma}'\right)=$$

$$\log_2\det\begin{pmatrix}\sum_{l\in\mathcal{N}_U}\mathbf{G}_{i,k}^{i}\tilde{\mathbf{U}}_{i,l}^{(S)}\mathbf{G}_{i,k}^{i\,\dagger}\\+\sum_{l\in\mathcal{N}_U}\mathbf{G}_{i,k}^{\bar{i}}\tilde{\mathbf{U}}_{\bar{i},l}^{(S)}\mathbf{G}_{i,k}^{\bar{i}\,\dagger}\\+\mathbf{H}_{i,k}^{i}(\mathbf{\Omega}_{i}^{(S)}+\mathbf{\Sigma}_{i}^{(S)})\mathbf{H}_{i,k}^{i\,\dagger}\\+\mathbf{H}_{i,k}^{\bar{i}}(\mathbf{\Omega}_{\bar{i}}^{(S)}+\mathbf{\Sigma}_{\bar{i}}^{(S)})\mathbf{H}_{i,k}^{\bar{i}\,\dagger}+\mathbf{I}\end{pmatrix}$$

$$-\frac{1}{\ln 2}\varphi\left(\begin{pmatrix}\sum_{l\in\mathcal{N}_U\setminus\{k\}}\mathbf{G}_{i,k}^{i}\tilde{\mathbf{U}}_{i,l}^{(S)}\mathbf{G}_{i,k}^{i\,\dagger}\\+\sum_{l\in\mathcal{N}_U}\mathbf{G}_{i,k}^{\bar{i}}\tilde{\mathbf{U}}_{\bar{i},l}^{(S)}\mathbf{G}_{i,k}^{\bar{i}\,\dagger}\\+\mathbf{H}_{i,k}^{i}(\mathbf{\Omega}_{i}^{(S)}+\mathbf{\Sigma}_{i}^{(S)})\mathbf{H}_{i,k}^{i\,\dagger}\\+\mathbf{H}_{i,k}^{\bar{i}}(\mathbf{\Omega}_{\bar{i}}^{(S)}+\mathbf{\Sigma}_{\bar{i}}^{(S)})\mathbf{H}_{i,k}^{\bar{i}\,\dagger}+\mathbf{I}\end{pmatrix},\begin{pmatrix}\sum_{l\in\mathcal{N}_U\setminus\{k\}}\mathbf{G}_{i,k}^{i}\tilde{\mathbf{U}}_{i,l}^{(S)\prime}\mathbf{G}_{i,k}^{i\,\dagger}\\+\sum_{l\in\mathcal{N}_U}\mathbf{G}_{i,k}^{\bar{i}}\tilde{\mathbf{U}}_{\bar{i},l}^{(S)\prime}\mathbf{G}_{i,k}^{\bar{i}\,\dagger}\\+\mathbf{H}_{i,k}^{i}(\mathbf{\Omega}_{i}^{(S)\prime}+\mathbf{\Sigma}_{i}^{(S)\prime})\mathbf{H}_{i,k}^{i\,\dagger}\\+\mathbf{H}_{i,k}^{\bar{i}}(\mathbf{\Omega}_{\bar{i}}^{(S)\prime}+\mathbf{\Sigma}_{\bar{i}}^{(S)\prime})\mathbf{H}_{i,k}^{\bar{i}\,\dagger}+\mathbf{I}\end{pmatrix}\right),$$

$$\hat{g}_{i,r}^{(i)}\left(\tilde{\mathbf{V}},\mathbf{\Omega},\tilde{\mathbf{V}}',\mathbf{\Omega}'\right)=$$

$$\frac{1}{\ln 2}\varphi\begin{pmatrix}\sum_{k\in\mathcal{N}_U}\mathbf{E}_{i,r}^{\dagger}\tilde{\mathbf{V}}_{i,k}^{(i)}\mathbf{E}_{i,r}+\mathbf{\Omega}_{i,r}^{(i)},\\\sum_{k\in\mathcal{N}_U}\mathbf{E}_{i,r}^{\dagger}\tilde{\mathbf{V}}_{i,k}^{(i)\prime}\mathbf{E}_{i,r}+\mathbf{\Omega}_{i,r}^{(i)\prime}\end{pmatrix}$$

$$-\log_2\det\left(\mathbf{\Omega}_{i,r}^{(i)}\right),$$

$$\hat{g}_{i,r}^{(S)}\left(\tilde{\mathbf{U}},\mathbf{\Omega},\tilde{\mathbf{U}}',\mathbf{\Omega}'\right)=$$

$$\frac{1}{\ln 2}\varphi\begin{pmatrix}\sum_{k\in\mathcal{N}_U}\tilde{\mathbf{E}}_{i,r}^{\dagger}\tilde{\mathbf{U}}_{i,k}^{(S)}\tilde{\mathbf{E}}_{i,r}+\mathbf{\Omega}_{i,r}^{(S)},\\\sum_{k\in\mathcal{N}_U}\tilde{\mathbf{E}}_{i,r}^{\dagger}\tilde{\mathbf{U}}_{i,k}^{(S)\prime}\tilde{\mathbf{E}}_{i,r}+\mathbf{\Omega}_{i,r}^{(S)\prime}\end{pmatrix}$$

$$-\log_2\det\left(\mathbf{\Omega}_{i,r}^{(S)}\right),$$

$$\hat{\gamma}_{i,r}^{(S)}\left(\tilde{\mathbf{U}},\mathbf{\Sigma},\tilde{\mathbf{U}}',\mathbf{\Sigma}'\right)=$$

$$\frac{1}{\ln 2}\varphi\begin{pmatrix}\sum_{k\in\mathcal{N}_U}\bar{\mathbf{E}}_{\bar{i},r}^{\dagger}\tilde{\mathbf{U}}_{\bar{i},k}^{(S)}\bar{\mathbf{E}}_{\bar{i},r}+\mathbf{\Sigma}_{i,r}^{(S)},\\\sum_{k\in\mathcal{N}_U}\bar{\mathbf{E}}_{\bar{i},r}^{\dagger}\tilde{\mathbf{U}}_{\bar{i},k}^{(S)\prime}\bar{\mathbf{E}}_{\bar{i},r}+\mathbf{\Sigma}_{i,r}^{(S)\prime}\end{pmatrix}$$

$$-\log_2\det\left(\mathbf{\Sigma}_{i,r}^{(S)}\right),$$

$$\hat{\beta}_{i,k,S}\left(\tilde{\mathbf{U}},\mathbf{\Sigma},\tilde{\mathbf{U}}',\mathbf{\Sigma}'\right)=$$

$$\frac{1}{\ln 2}\varphi\begin{pmatrix}\sum_{l\in\mathcal{N}_U}\bar{\mathbf{E}}_{i}^{\dagger}\tilde{\mathbf{U}}_{i,k}^{(S)}\bar{\mathbf{E}}_{i}+\mathbf{\Sigma}_{\bar{i}}^{(S)},\\\sum_{l\in\mathcal{N}_U}\bar{\mathbf{E}}_{i}^{\dagger}\tilde{\mathbf{U}}_{i,k}^{(S)\prime}\bar{\mathbf{E}}_{i}+\mathbf{\Sigma}_{\bar{i}}^{(S)\prime}\end{pmatrix}$$

$$-\log_2\det\left(\sum_{l\in\mathcal{N}_U\setminus\{k\}}\bar{\mathbf{E}}_{i}^{\dagger}\tilde{\mathbf{U}}_{i,k}^{(S)}\bar{\mathbf{E}}_{i}+\mathbf{\Sigma}_{\bar{i}}^{(S)}\right).$$

with the notations $\varphi(\mathbf{A},\mathbf{B})=\ln\det(\mathbf{B})+\mathrm{tr}(\mathbf{B}^{-1}(\mathbf{A}-\mathbf{B}))$, $\mathbf{G}_{i,k}^{j}=[\mathbf{H}_{i,k}^{j}\,\mathbf{H}_{i,k}^{\bar{j}}]$, $\tilde{\mathbf{E}}_{i,r}=[\mathbf{E}_{i,r}^{\dagger}\,\mathbf{0}_{n_{R,\bar{i}}\times n_{R,i,r}}^{\dagger}]^{\dagger}$, $\bar{\mathbf{E}}_{i,r}=[\mathbf{0}_{n_{R,i}\times n_{R,\bar{i},r}}^{\dagger}\,\mathbf{E}_{\bar{i},r}^{\dagger}]^{\dagger}$ and $\bar{\mathbf{E}}_{i}=[\mathbf{0}_{n_{R,i}\times n_{R,\bar{i}}}^{\dagger}\,\mathbf{I}_{n_{R,\bar{i}}}]^{\dagger}$.

REFERENCES

[1] A. Khan, W. Kellerer, K. Kozu, and M. Yabusaki, "Network sharing in the next mobile network: TCO reduction, management flexibility, and operational independence," *IEEE Commun. Mag.*, vol. 49, no. 10, pp. 134–142, Oct. 2011.

[2] E. A. Jorswieck, L. Badia, T. Fahldieck, E. Karipidis, and J. Luo, "Spectrum sharing improves the network efficiency for cellular operators," *IEEE Commun. Mag.*, vol. 52, no. 3, pp. 129–136, Mar. 2014.

[3] K. Samdanis, X. Costa-Perez, and V. Sciancalepore, "From network sharing to multitenancy: The 5G network slicer broker," *IEEE Commun. Mag.*, vol. 54, no. 7, pp. 32–39, Jul. 2016.

[4] F. Boccardi *et al.*, "Spectrum pooling in mmWave networks: Opportunities, challenges, and enablers," *IEEE Commun. Mag.*, vol. 54, no. 11, pp. 33–39, Nov. 2016.

[5] O. Aydin, E. A. Jorswieck, D. Aziz, and A. Zappone, "Energy-spectral efficiency tradeoffs in 5G multioperator networks with heterogeneous constraints," *IEEE Trans. Wireless Commun.*, vol. 16, no. 9, pp. 5869–5881, Sep. 2017.

[6] J. Park, J. G. Andrews, and R. W. Heath Jr., "Interoperator base station coordination in spectrum-shared millimeter wave cellular networks," *IEEE Trans. Cogn. Commun. Netw.*, vol. 4, no. 3, pp. 513–528, Sep. 2018.

[7] X. Foukas, G. Patounas, A. Elmokashfi, and M. K. Marina, "Network slicing in 5G: Survey and challenges," *IEEE Commun. Mag.*, vol. 55, no. 5, pp. 94–100, May 2017.

[8] O. Simeone, A. Maeder, M. Peng, O. Sahin, and W. Yu, "Cloud radio access network: Virtualizing wireless access for dense heterogeneous systems," *J. Commun. Netw.*, vol. 18, no. 2, pp. 135–149, Apr. 2016.

[9] T. Q. Quek, M. Peng, O. Simeone, and W. Yu, *Cloud Radio Access Networks: Principles, Technologies, and Applications*. Cambridge, U.K.: Cambridge Univ. Press, Apr. 2017.

[10] O. Simeone, O. Somekh, H. V. Poor, and S. Shamai (Shitz), "Downlink multicell processing with limited-backhaul capacity," *EURASIP J. Adv. Signal Process.*, vol. 2009, no. 3, pp. 1–10, Jun. 2009.

[11] S.-H. Park, O. Simeone, O. Sahin, and S. Shamai (Shitz), "Joint precoding and multivariate backhaul compression for the downlink of cloud radio access networks," *IEEE Trans. Signal Process.*, vol. 61, no. 22, pp. 5646–5658, Nov. 2013.

[12] S.-H. Park, O. Simeone, O. Sahin, and S. Shamai (Shitz),"Fronthaul compression for cloud radio access networks: Signal processing advances inspired by network information theory," *IEEE Signal Process. Mag.*, vol. 31, no. 6, pp. 69–79, Nov. 2014.

[13] M. Tao, E. Chen, H. Zhou, and W. Yu, "Content-centric sparse multicast beamforming for cache-enabled cloud RAN," *IEEE Trans. Wireless Commun.*, vol. 15, no. 9, pp. 6118–6131, Sep. 2016.

[14] W. Lee, O. Simeone, J. Kang, and S. Shamai (Shitz),"Multivariate fronthaul quantization for downlink C-RAN," *IEEE Trans. Signal Process.*, vol. 64, no. 19, pp. 5025–5037, Oct. 2016.

[15] S.-H. Park, O. Simeone, and S. Shamai (Shitz), "Joint optimization of cloud and edge processing for fog radio access networks," *IEEE Trans. Wireless Commun.*, vol. 15, no. 11, pp. 7621–7632, Nov. 2016.

[16] L. Liu and W. Yu, "Cross-layer design for downlink multihop cloud radio access networks with network coding," *IEEE Trans. Signal Process.*, vol. 65, no. 7, pp. 1728–1740, Apr. 2017.

[17] S.-H. Park, O. Simeone, O. Sahin, and S. Shamai (Shitz), "Robust and efficient distributed compression for cloud radio access networks," *IEEE Trans. Veh. Technol.*, vol. 62, no. 2, pp. 692–703, Feb. 2013.

[18] Y. Zhou, Y. Xu, W. Yu, and J. Chen, "On the optimal fronthaul compression and decoding strategies for up link cloud radio access networks," *IEEE Trans. Inf. Theory*, vol. 62, no. 2, pp. 7402–7418, Dec. 2016.

[19] X. He and A. Yener, "Cooperation with an untrusted realy: A secrecy perspective," *IEEE Trans. Inf. Theory*, vol. 56, no. 8, pp. 3807–3827, Aug. 2010.

[20] R. Bassily *et al.*, "Cooperative security at the physical layer," *IEEE Signal Process. Mag.*, vol. 30, no. 5, pp. 16–28, Sep. 2013.

[21] W. K. Harrison and S. W. McLaughlin, "Physical-layer security: Combining error control coding and cryptography," in *Proc. IEEE Int. Conf. Commun.*, Dresden, Germany, Jun. 2009, pp. 1–5.

[22] M. Vincenzi, A. Antonopoulos, E. Kartsakli, J. Vardakas, L. Alonso, and C. Verikoukis, "Multitenant slicing for spectrum management on the road to 5G," *IEEE Wireless Commun.*, vol. 24, no. 5, pp. 118–125, Oct. 2017.

[23] C. Raman, R. D. Yates, and N. B. Mandayam, "Scheduling variable rate links via a spectrum server," in *Proc. 1st IEEE Symp. New Frontiers Dyn. Spectr. Access Netw.*, Baltimore, MD, USA, Nov. 2005, pp. 110–118.

[24] O. Ileri, D. Samardzija, and N. Mandayam, "Demand responsive pricing and competitive spectrum allocation via a spectrum servier," in *Proc. 1st IEEE Symp. New Frontiers Dyn. Spectr. Access Netw.*, Baltimore, MD, USA, Nov. 2005, pp. 194–202.
[25] A. Goldsmith, S. A. Jafar, N. Jindal, and S. Vishwanath, "Capacity limits of MIMO channels," *IEEE J. Sel. Areas Commun.*, vol. 21, no. 5, pp. 684–702, Jun. 2003.
[26] Y. Shi, J. Zhang, and K. B. Letaief, "Robust group sparse beamforming for multicast green cloud-RAN with imperfect CSI," *IEEE Trans. Signal Process.*, vol. 63, no. 17, pp. 4647–4659, Sep. 2015.
[27] S. Jeong, O. Simeone, and J. Kang, "Optimization of massive full-dimensional MIMO for positioning and communication," *IEEE Trans. Wireless Commun.*, vol. 17, no. 9, pp. 6205–6217, Sep. 2018.
[28] Y. Saito, Y. Kishiyama, A. Benjebbour, T. Nakamura, A. Li, and K. Higuchi, "Nonorthogonal multiple access (NOMA) for cellular future radio access," in *Proc. IEEE Veh. Technol. Conf.*, Dresden, Germany, Jun. 2013, pp. 1–5.
[29] W. Shin, M. Vaezi, B. Lee, D. J. Love, J. Lee, and H. V. Poor, "Nonorthogonal multiple access in multicell networks: Theory, performance, and practical challenges," *IEEE Commun. Mag.*, vol. 55, no. 10, pp. 176–183, Oct. 2017.
[30] E. Chen, M. Tao, and Y.-F. Liu, "Joint base station clustering and beamforming for nonorthogonal multicast and unicast transmission with backhaul constraints," *IEEE Trans. Wireless Commun.*, vol. 17, no. 9, pp. 6265–6279, Sep. 2018.
[31] J. Ostergaard and R. Zamir, "Multiple-description coding by dithered delta-sigma quantization," *IEEE Trans. Inf. Theory*, vol. 55, no. 10, pp. 4661–4675, Oct. 2009.
[32] A. E. Gamal and Y.-H. Kim, *Network Information Theory*. Cambridge, U.K.: Cambridge Univ. Press, 2011.
[33] I. Csiszar and J. K. Korner, *Information Theory: Coding Theorems for Discrete Memoryless Systems*. London, U.K.: Academic, 1981.
[34] M. Grant and S. Boyd, "CVX: Matlab software for disciplined convex programming," ver 2.0 beta, Sep. 2013. [Online]. Available: http://cvxr.com/cvx
[35] S. Boyd and L. Vandenberghe, *Convex Optimization*. Cambridge, U.K.: Cambridge Univ. Press, 2004.
[36] D. P. Palomar and M. Chiang, "A tutorial on decomposition methods for network utility maximization," *IEEE J. Sel. Areas Commun.*, vol. 24, no. 8, pp. 1439–1451, Aug. 2006.

Seok-Hwan Park (M'11) received the B.Sc. and Ph.D. degrees in electrical engineering from Korea University, Seoul, South Korea, in 2005 and 2011, respectively.

Since 2015, he has been with Chonbuk National University (CBNU), Jeonsu, South Korea, as an Assistant Professor. Prior to joining CBNU, he was with New Jersey Institute of Technology and Samsung Electronics. His research interests include MIMO communications, optimization theory, and machine learning. He was the recipient of the Best Paper Award at the 2006 Asia-Pacific Conference on Communications and an Excellent Paper Award at IEEE Student Paper Contest in 2006.

Osvaldo Simeone (F'16) received the M.Sc. degree (with Hons.) and the Ph.D. degree in information engineering from Politecnico di Milano, Milan, Italy, in 2001 and 2005, respectively. He is currently a Professor of information engineering with the Centre for Telecommunications Research, Department of Informatics, King's College London, London, U.K. From 2006 to 2017, he was a faculty member of the Electrical and Computer Engineering Department, New Jersey Institute of Technology, where he was with the Center for Wireless Information Processing. He is a co-author of two monographs, an edited book published by Cambridge University Press, and more than one hundred research journal papers. His research interests include wireless communications, information theory, optimization, and machine learning. He is a co-recipient of the 2017 JCN Best Paper Award, the 2015 IEEE Communication Society Best Tutorial Paper Award, and of the Best Paper Awards of IEEE SPAWC 2007 and IEEE WRECOM 2007. He was awarded a Consolidator grant by the European Research Council (ERC) in 2016. His research has been supported by the U.S. NSF, the ERC, the Vienna Science and Technology Fund, as well by a number of industrial collaborations. He is currently on the editorial board of the IEEE SIGNAL PROCESSING MAGAZINE, and is a Distinguished Lecturer of the IEEE Information Theory Society. He is a Fellow of the IET.

Shlomo Shamai (Shitz) (F'94) received the B.Sc., M.Sc., and Ph.D. degrees in electrical engineering from the Technion—Israel Institute of Technology, Haifa, Israel, in 1975, 1981, and 1986, respectively.

During 1975–1985, he was with the Communications Research Laboratory, as a Senior Research Engineer. Since 1986, he has been with the Department of Electrical Engineering, Technion—Israel Institute of Technology, where he is now a Technion Distinguished Professor and the William Fondiller Chair of telecommunications. His research interests encompasses a wide spectrum of topics in information theory and statistical communications.

Dr. Shamai (Shitz) is the recipient of the 2011 Claude E. Shannon Award, the 2014 Rothschild Prize in Mathematics/Computer Sciences and Engineering and the 2017 IEEE Richard W. Hamming Medal. He has been awarded the 1999 van der Pol Gold Medal of the Union Radio Scientifique Internationale (URSI), and is a co-recipient of the 2000 IEEE Donald G. Fink Prize Paper Award, the 2003 and 2004 joint IT/COM societies paper award, the 2007 IEEE Information Theory Society Paper Award, the 2009 and 2015 European Commission FP7, Network of Excellence in Wireless COMmunications (NEWCOM++, NEWCOM#) Best Paper Awards, the 2010 Thomson Reuters Award for International Excellence in Scientific Research, the 2014 EURASIP Best Paper Award (for the EURASIP Journal on Wireless Communications and Networking), and the 2015 IEEE Communications Society Best Tutorial Paper Award. He is also the recipient of 1985 Alon Grant for distinguished young scientists and the 2000 Technion Henry Taub Prize for Excellence in Research. He was an Associate Editor for the Shannon Theory of the IEEE TRANSACTIONS ON INFORMATION THEORY, and also on the Board of Governors of the Information Theory Society. He was also on the Executive Editorial Board of the IEEE TRANSACTIONS ON INFORMATION THEORY and the IEEE Information Theory Society Nominations and Appointments Committee. He is an URSI Fellow, a member of the Israeli Academy of Sciences and Humanities, and a foreign member of the US National Academy of Engineering.